NON-REVERSAL OPEN QUANTUM WALKS

By

GOOLAM HOSSEN Yashine Hazmatally

Dissertation Submitted in Fulfillment
of the Academic Requirements
for the Degree of MSc Physics
in the School of Chemistry and Physics
University of KwaZulu-Natal, Westville Campus
Durban, South Africa
December 2015

As the candidate's supervisors, we have approved this dissertation for submission.

Name: _____ Signed: _____ Date: _____

Name: _____ Signed: _____ Date: _____

Abstract

In this thesis, a new model of non-reversal quantum walk is proposed. In such a walk, the walker cannot go back to previously visited sites but it can stay static or move to a new site. The process is set up on a line using the formalism of Open Quantum Walks (OQWs). Afterwards, non-reversal quantum trajectories are launched on a 2-D lattice to which a memory is associated to record visited sites. The "quantum coins" are procured from a randomly generated unitary matrix. The radius of spread of the non-reversal OQW varies with different unitary matrices. The statistical results have meaningful interpretations in polymer physics. The number of steps of the trajectories is equivalent to the degree of polymerization, N. The root-mean-square of the radii determines the end-to-end distance, R of a polymer. These two values being typically related by $R \sim N^{\nu}$, the critical exponent, ν, is obtained for $N \leq 400$. It is found to be closely equal to the Flory exponent. However, for larger N, the relationship does not hold anymore. Hence, a different relationship between R and N is suggested.

UNIVERSITY OF KWAZULU-NATAL, WESTVILLE CAMPUS

Author: **GOOLAM HOSSEN Yashine Hazmatally**

Title: **Non-reversal Open Quantum Walks**

The work described in this dissertation was carried out in the School of Chemistry and Physics, University of KwaZulu-Natal, Westville Campus, Durban, from January 2014 to December 2015, under the supervision of Professor Francesco Petruccione and Dr. Ilya Sinayskiy.

These studies represent original work by the author and have not otherwise been submitted in any form for any degree or diploma to any tertiary institution. Where use has been made of the work of others it is duly acknowledged in the text.

The financial assistance of the National Research Foundation (NRF) towards this research is hereby acknowledged. Opinions expressed and conclusions arrived at, are those of the author and are not necessarily to be attributed to the NRF.

_____

Signature of Author

UNIVERSITY OF KWAZULU-NATAL, WESTVILLE CAMPUS

Declaration - Plagiarism

I, _____

declare that

i. The research reported in this thesis, except where otherwise indicated, is my original research.

ii. This thesis has not been submitted for any degree or examination at any other university.

iii. This thesis does not contain other persons' data, pictures, graphs or other information, unless specifically acknowledged as being sourced from other persons.

iv. This thesis does not contain other persons' writing, unless specifically acknowledged as being sourced from other researchers. Where other written sources have been quoted, then:
a. Their words have been re-written but the general information attributed to them has been referenced;
b. Where their exact words have been used, their writing has been placed inside quotation marks, and referenced.

v. This thesis does not contain text, graphics or tables copied and pasted from the Internet, unless specifically acknowledged, and the source being detailed in the thesis and in the References sections.

Date:_____ _____
Author

Supervisor: _____
Professor Francesco Petruccione

Co-supervisor: _____
Dr. Ilya Sinayskiy

Conferences & Publication

During my Master's study, I attended the following workshops and conferences. At most of them, I presented my work, which lead to fruitful interactions with research experts in related fields. Some of the researchers were the authors of the papers I studied to develop the thesis.

Name: Quantum Information, Processing, Communication and Control (QIPCC 2)
Date: 25 to 29 November, 2013
Venue: Pumula Beach Hotel, in South Coast of KZN, South Africa

Name: School in Physics on Coherent Quantum Dynamics (CQD)
Date: 16 to 25 September 2014
Venue: OIST in Okinawa, Japan
Presentation type: Poster
Title: Quantum self-avoiding walks

Name: Postgraduate Research Day
Date: 27 October 2014
Venue: UKZN, Westville campus, Durban, South Africa
Presentation type: Poster
Title: Open quantum self-avoiding walks

Name: Quantum Information, Processing, Communication and Control (QIPCC 3)
Date: 3 to 7 November 2014
Venue: Alpine Heath in Drakensberg, South Africa
Presentation type: Oral
Title: Open quantum self-avoiding walks

Name: Quantum Simulations and Quantum Walks (QSQW)
Date: 24 to 28 November 2014
Venue: Pumula Beach Hotel, in South Coast of KZN,, South Africa
Presentation type: Oral
Title: Open quantum self-avoiding walks

Name: CHPC National Meeting and Conference
Date: 1 to 5 December 2014
Venue: Kruger National Park, South Africa
Presentation type: Poster
Title: Open quantum self-avoiding walks

Name: Workshop in Quantum Physics: Foundations and Applications
Date: 3 to 13 February 2015
Venue: STIAS (NITheP), Stellenbosch, South Africa
Presentation type: Oral
Title: Open quantum self-avoiding walks

Name: Postgraduate Research Day
Date: 22 September 2015
Venue: UKZN, Pietermaritzburg campus, Pietermaritzburg, South Africa
Presentation type: Oral
Title: Non-reversal Open Quantum Walks

Name: Quantum Research Theoretical Group Meeting
Date: 29 September 2015, 23 November 2015
Venue: UKZN, Westville campus, Durban, South Africa
Presentation type: Oral and intensive discussion
Title: Non-reversal Open Quantum Walks

Publication

Goolam Hossen, Y.H., Sinayskiy, I. and Petruccione, F., 2015. Non-reversal open quantum walks. in preparation.

Acknowledgements

"Behind everything there is science." *M̃aster Taner*

The accomplishment of this thesis is thanks to the kindness and patience of my supervisor, Professor Francesco Petruccione, and co-supervisor, Dr. Ilya Sinayskiy. The support of my former co-supervisor, Dr. F. Giraldi, and colleague, Dr. R. Caballar, is also appreciated. Furthermore, I am grateful to all my other colleagues in the Quantum Research Group who assisted me directly or indirectly.

For the technical support, I would like to acknowledge Professor Jonathan Sievers for providing access to the cluster Hippo. To get familiar with Hippo, the generous assistance of Dr. S. Muya Kasanda and Mr. Bryan Johnston from the School of Mathematics, Statistics and Computer Science was valuable.

To sum up, I would like to express gratitude to the School of Chemistry and Physics, to UKZN as a whole and to the National Research Foundation (N.R.F) for generously funding this research work. A big thanks goes to the sponsors of the conferences and workshops I attended, especially the National Institute of Theoretical Physics (NITheP). I had the privilege to meet research experts. I am thankful for their contribution through valuable interaction and questions.

Finally we thank you reader and hope you enjoy the thesis!

Love and Peace to you all in the Space of Unity

To our family

Table of Contents

Notations

$\mathcal{H}, \mathcal{K}$	:	Hilbert space
$\mathbf{B}(\mathcal{H})$	:	Set of bounded operators on $\mathcal{H}$
$\hbar$	:	Reduced Planck constant
t	:	time
$\|\psi\rangle$	:	state vector
$\langle .\|.\rangle$	:	inner product in $\mathcal{H}$
$\|.\rangle\langle .\|$	:	outer product in $\mathcal{H}$
$\otimes$	:	tensor product
$\|\|.\|\|$	:	Norm in $\mathcal{H}$ unless specified differently
Tr	:	Trace
$.^{\dagger}$	:	adjoint
$.^{-1}$	:	inverse
U	:	Unitary operator
I	:	Identity operator
$\frac{d}{dt}$	:	differentiation with respect to time
$[A, B]$	:	$= AB - BA$

Abbreviations

$1D$	:	one-dimension
$2D$	:	two-dimension
SAW	:	Self-Avoiding Walk
OQW	:	Open Quantum Walk

Chapter 1

Introduction

"*Avoiding yourself, it turns out, is a hard problem.*" [1]

A random walk is a process in which an object (a particle) moves randomly. Random walks are known to have been used since 1880 by Rayleigh in modeling a sound wave through a material. However, only 20 years later, the theory of random walks was proposed by Louis Bachelier through his thesis "La Théorie de la Spéculation" [2]. His objective was to express and predict stock market behaviour. The term "random walk" was introduced by Karl Pearson in 1905 through a description of mosquito infestation in a forest. Surprisingly, in the same year, the famous publication on Brownian motion by Albert Einstein came out [3]. It became the major contribution to random walks. Another such independent work was published by M. Smoluchowski in 1906 [4].

Almost after half a century, scientists started showing interest to the self-avoiding version of the random walk. Since then, the Self-Avoiding Walk (SAW) has been an active area of research. Basically, it is a random walk whereby the object cannot go back to an already visited site of its path. This definition has been convenient especially to chemists [5, 6] as it makes the SAWs one of the main mechanism that can be used to model the growth of crystals and polymers [7]. The Nobel prize winner, Paul J. Flory, came up with an exact formula that characterises the properties of a typical SAW which has been verified numerically [8]. Recently the Flory conjecture was proven in 2D [9]. As a result, SAWs have become of equal importance to mathematicians. The classical SAW is being studied on $\mathbb{Z}^2$ and on the honeycomb (hexagonal) lattice [10]. It has also been analysed numerically on other two-dimensional ($2D$)

lattices [11]. However, there are some analytical questions about the classical SAW that remain unsolved so far.

Recently, some types of SAWs have been implemented as unitary quantum walks [12]. They were called the non-reversal quantum walks and non-repeating quantum walks [13]. Unfortunately, such quantum walks cannot be completely self-avoiding due to the unitary dynamics of the system [14]. Consequently, a setup of non-reversal walk, using the non-unitary formalism of an open quantum system [15], is attempted. The Open Quantum Walk (OQW) has the properties of both classical random walks and unitary quantum walks [16]. After a careful study of these properties, the non-reversal OQW is formulated.

The structure of the thesis consists of four main parts.

In Chapter 2, the necessary mathematical formalism is introduced. This includes the Hilbert space and the Dirac notation of vectors in that space [17]. The axioms of quantum mechanics are enumerated in terms of the density operator [18]. The unitary operators are also introduced since they describe the evolution of a closed quantum system. Chapter 2 is concluded with an explanation of the open quantum system, whereby decoherence due to the external environment (or the observer) is taken into consideration.

Chapter 3 revolves around the different types of random walks. The classical SAW is defined and implemented on the cartesian plane. Subsequently, quantum walks are reviewed, especially the Grover walk [19], the non-reversal and non-repeating quantum walks [13]. They are different with respect to their coin operators. However, the same step operator is employed for all of them. Both the coin and the step operators are unitary (hence the walks are referred as unitary quantum walks). Lastly, the Open Quantum Walk on a two-dimensional lattice is described meticulously. Its mathematical formalism is adapted from [16]. The probability distributions of the OQW in one dimension and two dimension are analysed.

In the fourth chapter, the trivial case of non-reversal OQW is formulated using the principle of quantum trajectories. A memory system is associated with the number line on which the walk takes place. Then, the memory setup is extended to the cartesian plane for the formulation of the two-dimensional version of the walk. Different

distributions of non-reversal OQWs are produced by varying the choice of Kraus operators. The radii of spread of the non-reversal walks is analysed with respect to the different Kraus operators used. The statistical results are applied in the field of polymer physics [20] such that the universal critical exponent can be determined. This is done for the ordinary OQW too.

To conclude, a new formula is suggested for the relationship between the end-to-end distance of a polymer and its degree of polymerisation. This gives rise to many open questions that will be investigated in the near future. Other possible prospects of the suggested model of non-reversal OQWs are also considered. It is speculated that the non-reversal OQW could be useful in quantum simulations due to its characteristic of dispersion. This property could make it suitable for search algorithm as well. Finally, it has been claimed in [21] that random walks are expected to benefit in the development of quantum algorithms which are fundamental for a conceivable quantum computer [22]. However, before reaching this stage, the non-reversal OQW demands further analysis which therefore opens up a wide range of studying opportunities.

Chapter 2

The Quantum World

To admire the beauty of the world at the quantum scale, one first needs a notion of the quantum system. The aim of this chapter is to introduce the mathematical language in which this system is set up. We shall cover the preliminary linear operators acting on the Hilbert space as well as their properties [17]. Subsequently, we shall list the axioms of quantum mechanics and introduce the open quantum system.

A **Hilbert space** is a complete inner-product complex vector space. Later, we shall demonstrate the role of the vector space in the enumeration of the axioms of quantum mechanics. The Hilbert space is also an appropriate setting for probability theory. Some physicists view quantum mechanics as being the probability theory of nature. Dirac was one of them. Let us proceed with one of his contributions to the language of quantum physics.

2.1 The Dirac Notation

Let $\mathcal{H}$ be a Hilbert space. A vector, $|\psi\rangle \in \mathcal{H}$, is called a **ket**. The corresponding linear functional, which is an element of the dual space of $\mathcal{H}$, is denoted as $\langle\psi|$ and is called **bra**. Thus, $\langle .|$ can be seen as a linear transformation that maps each state ϕ into a functional $\langle\phi|$ such that

$$\langle\phi|(|\psi\rangle) = \langle\phi|\psi\rangle.$$

We further define the **norm** of ψ,

$$\|\psi\| = \sqrt{\langle\psi|\psi\rangle}.$$

Next, we introduce the mathematical operators which are necessary tools in quantum physics.

2.2 Linear Operators

Let $\mathcal{H}_1$ and $\mathcal{H}_2$ be Hilbert spaces. Then, a linear transformation, $\hat{B} \in \mathbf{B}(\mathcal{H}_1, \mathcal{H}_2)$, over the field of $\mathbb{C}$, is a mapping from $\mathcal{H}_1$ to $\mathcal{H}_2$ such that $\forall\ |\psi\rangle_i \in \mathcal{H}_1, \alpha_j \in \mathbb{C}$,

$$\hat{B}\left(\sum_m \alpha_m |\psi\rangle_m\right) = \sum_m \alpha_m \hat{B}(|\psi\rangle_m) = \sum_m \alpha_m |\phi\rangle_m, \text{ with } |\phi\rangle_m \in \mathcal{H}_2.$$

When $\mathcal{H} = \mathcal{H}_1 = \mathcal{H}_2$, then the transformation is called a **linear operator**. Furthermore, $\hat{B}$ is said to be **bounded** if there exists $M > 0$ such that $\forall\ |\psi\rangle_i \in \mathcal{H}_1$,

$$\|\hat{B}(|\psi\rangle_i)\|_{\mathcal{H}_2} \leq M \||\psi\rangle_i\|_{\mathcal{H}_1}.$$

$\forall\ |v\rangle, |w\rangle \in \mathcal{H}$, given any linear operator $A \in \mathbf{B}(\mathcal{H})$, there exists an **adjoint**, $A^\dagger$ such that

$$\langle A^\dagger v | w\rangle = \langle w | Av\rangle.$$

Example: Let A be a four by four matrix which represents a linear operator on $\mathbb{C}^4$ with complex entries as follows.

$$A = \begin{pmatrix} a & b & c & d \\ e & f & g & h \\ i & j & k & l \\ m & n & o & p \end{pmatrix}.$$

Then, its adjoint is given by

$$A^\dagger = \begin{pmatrix} a^* & e^* & i^* & m^* \\ b^* & f^* & j^* & n^* \\ c^* & g^* & k^* & o^* \\ d^* & h^* & l^* & p^* \end{pmatrix},$$

where a^* is the complex conjugate of a, b^* is the complex conjugate of b, ...

A is called a **self-adjoint** operator if $A = A^\dagger$. In the case of finite dimensional Hilbert space ($\mathcal{H} = \mathbb{C}^n$), the typical example of such an operator is the *Hamiltonian* of the system.

Let us look at the operators which will be crucial in the formulation of unitary quantum walks.

2.2.1 Unitary operators

U is **unitary** if its adjoint is equal to its inverse,

$$U^\dagger = U^{-1}.$$

An example of a unitary matrix is the Hadamard matrix on $\mathbb{C}^2$,

$$H = \frac{1}{\sqrt{2}} \begin{pmatrix} 1 & 1 \\ 1 & -1 \end{pmatrix}. \tag{2.2.1}$$

A unitary operator preserves length and the angle between vectors. This will ensure that the conservation of probability is achieved. Moreover, given that U is unitary, then $U^\dagger$ is also unitary such that

$$U^\dagger U = U U^\dagger = I.$$

The next operator that we introduce will play a key role in the implementation of the *Open Quantum Walk* in Chapter 3.

2.2.2 Density operators

When the state of a quantum system can be described with a single vector from the Hilbert space, it is called a **pure state**. Otherwise, it is referred as **mixed quantum state**.

Let a quantum system be described by a vector $|\psi_i\rangle$ with probability p_i for some i. The set of these possible quantum states $\{p_i, |\psi_i\rangle\}$ is called an ensemble of pure states. Then, the **density operator** is defined as

$$\rho \equiv \sum_i p_i |\psi_i\rangle\langle\psi_i|. \tag{2.2.2}$$

We observe that ρ is not unique since it can be defined by different ensembles of quantum states. For a pure state, the density matrix is always given by

$$\rho \equiv |\psi\rangle\langle\psi|.$$

Since $|\psi_i\rangle$ are pure states, Equation (2.2.2) can be rewritten as

$$\rho \equiv \sum_i p_i \rho_i,$$

where

$$\rho_i \equiv |\psi_i\rangle\langle\psi_i|.$$

Properties of density operators

Density operators have intrinsic characteristics. Before looking at them, we need to understand what is meant by trace.

For a given matrix $A = \{a_{ij}\}_{i,j}^N$, the **trace** is stated as

$$\mathrm{Tr}(A) = \sum_{i=1}^{N} a_{ii}.$$

The two types of state we came across can be distinguished since

$$\mathrm{Tr}(\rho^2) \begin{cases} = 1, \text{ for pure state;} \\ < 1, \text{ for mixed state.} \end{cases}$$

Another property of ρ is that it is *Hermitian*, that is,

$$\rho = \rho^\dagger.$$

Furthermore, given that $\mathcal{K}$ is a Hilbert space. Then, an operator, $\rho \in \mathbf{B}(\mathcal{K})$, is the density operator associated to some ensemble $\{p_i, |\psi_i\rangle\}$ if and only if

1. $\mathrm{Tr}(\rho) = 1$ **(conservation of probability condition)**;
2. $\forall |\varphi\rangle \in \mathcal{K}, \langle\varphi|\rho|\varphi\rangle \geq 0$ **(positivity condition)**.

With the help of the above characterization, we can list the axioms of quantum mechanics accordingly.

2.3 Postulates of Quantum Mechanics

The foundation of Quantum Physics lies upon four fundamental axioms. These axioms expresses the physical quantum world into a mathematical language. Usually, the postulates are described in terms of pure state of a quantum system. In our context, we choose the description in terms of density operators from [18].

Postulate 1: A *Hilbert space* can be associated with any isolated physical system. It is referred as the state space of the system. The density operator, ρ acts on this space and describes completely the quantum system in the state ρ_i with probability p_i.

Postulate 2: A unitary transformation sets forth the evolution of a closed quantum system. This means that the state ρ of the system at time t_1 is related to the state ρ' of the system at time t_2 by a unitary operator U which depends only on the times t_1 and t_2;

$$\rho'(t_2) = U(t_2, t_1)\rho(t_1)U^\dagger(t_2, t_1).$$

Postulate 3: The quantum measurements are specified by a collection of measurement operators $\{M_m\}$ acting on the state space of the system being measured. The index m refers to the possible measurement outcomes in the experiment.
Given that the state of the quantum system is ρ just before the measurement is made, then the probability that result m occurs,

$$p(m) = \mathrm{Tr}(M_m^\dagger M_m \rho),$$

and the state of the system after the measurement is

$$\frac{M_m \rho M_m^\dagger}{\mathrm{Tr}(M_m^\dagger M_m \rho)}.$$

The full set of measurement operators satisfies the completeness equation,

$$\sum_m M_m^\dagger M_m = I.$$

Postulate 4: The state space of a composite physical system is the tensor product of the state spaces of the component physical systems. Let ρ_i be the state of quantum systems for $i = 1, ...n$, then the joint state of the total system is given by

$$\rho_1 \otimes \rho_2 \otimes ...\rho_n.$$

Postulate 4 will help in the study of subsystems of a composite quantum system. Such a system emphasizes a crucial part of the thesis. Let us elaborate on it.

2.4 Quantum Systems

Consider the **Schrödinger equation**,

$$i\hbar\frac{d}{dt}|\psi(t)\rangle = \mathrm{H}(t)|\psi(t)\rangle, \tag{2.4.1}$$

where H is the *Hamiltonian* of the system (In the remaining part of the thesis, it is assumed that we are working in the system of units where the reduced Planck constant, $\hbar$, is equal to one). Its solution,

$$U(t, t_0) = e^{-i\mathrm{H}(t-t_0)}, \tag{2.4.2}$$

governs the evolution of a state vector, $|\psi(t)\rangle$ of a **closed** physical system.

It is very difficult to isolate a particular closed quantum system. As a result, we have to face *decoherence* which arises due to the presence of an external system (the environment or the "observer"). This phenomenon is a current obstacle to the realisation of a quantum computer. In order to present the formalism of the open system, the following tool is essential.

2.4.1 Partial trace

The definition below is an extension to Equation (2.2.2) that helps in describing open quantum systems.

Let $\mathcal{A}$ and $\mathcal{B}$ be two physical systems whose joint state is represented by a density operator $\rho_{\mathcal{AB}}$. Let $|\alpha_1\rangle, |\alpha_2\rangle \in \mathcal{H}_{\mathcal{A}}$ and $|\beta_1\rangle, |\beta_2\rangle \in \mathcal{H}_{\mathcal{B}}$. Then, the **reduced density operator** for system $\mathcal{A}$ is defined as

$$\rho_{\mathcal{A}} \equiv \mathrm{Tr}_{\mathcal{B}} \left(\rho_{\mathcal{AB}}\right), \tag{2.4.3}$$

where $\mathrm{Tr}_{\mathcal{B}}$ is called the **partial trace** over system $\mathcal{B}$ and is given by

$$\mathrm{Tr}_{\mathcal{B}}(|\alpha_1\rangle\langle\alpha_2| \otimes |\beta_1\rangle\langle\beta_2|) \equiv |\alpha_1\rangle\langle\alpha_2|\mathrm{Tr}(|\beta_1\rangle\langle\beta_2|) \equiv |\alpha_1\rangle\langle\alpha_2|\langle\beta_2|\beta_1\rangle.$$

2.4.2 Open quantum systems

"*Quantum mechanics in itself involves an intimate relationship to the notion of an open system through the action of the measurement process.*" [15]

When two quantum systems (the principal system and the environment as shown in Figure 2.1) are combined, then the subsystem being observed, is said to be **open** given that the total combined system is closed and follows Hamiltonian dynamics. Hence, the formulation of quantum mechanics in terms of the statistical operator, ρ defined in section 2.2.2, becomes helpful.

The fact that the open system is in a *mixed state*, the corresponding equation of motion for the density operator ρ is given by the **Liouville-von Neumann equation**,

$$\frac{d}{dt}\rho(t) = -i\ [\mathrm{H}_{\mathrm{tot}}, \rho(t)], \tag{2.4.4}$$

where the total Hamiltonian of this system is expressed as

$$\mathrm{H}_{\mathrm{tot}} = \mathrm{H}_{\mathrm{sys}} + \mathrm{H}_{\mathrm{env}} + \mathrm{H}_{\mathrm{int}},$$

such that the Hamiltonians:

$\mathrm{H}_{\mathrm{sys}} \in \mathbf{B}(\mathcal{H}_{\mathcal{A}} \otimes \mathcal{I}_{\mathcal{B}})$ is for the system,

$\mathrm{H}_{\mathrm{env}} \in \mathbf{B}(\mathcal{I}_{\mathcal{A}} \otimes \mathcal{H}_{\mathcal{B}})$ is for the environment,

$\mathrm{H}_{\mathrm{int}} \in \mathbf{B}(\mathcal{H}_{\mathcal{A}} \otimes \mathcal{H}_{\mathcal{B}})$ is for the interaction between the system and the environment.

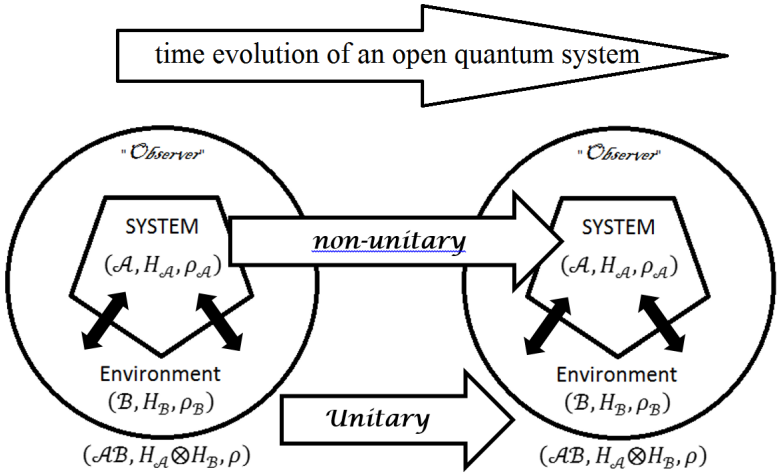

Figure 2.1: The evolution of a total quantum system $\mathcal{AB}$, which is composed of a system $\mathcal{A}$, coupled to the environment (or the observer) $\mathcal{B}$. $\mathcal{H}_{\mathcal{A}} \otimes \mathcal{H}_{\mathcal{B}}, \mathcal{H}_{\mathcal{A}} \otimes \mathcal{I}_{\mathcal{B}}$ and $\mathcal{I}_{\mathcal{A}} \otimes \mathcal{H}_{\mathcal{B}}$ are their respective Hilbert spaces; $\rho, \rho_{\mathcal{A}}$ and $\rho_{\mathcal{B}}$ are the respective density states of the systems. While the total system is assumed to be closed and therefore has a unitary evolution, the principal system has a non-unitary evolution when the environment is traced out. (Adapted from [15])

The solution of Equation (2.4.4) is given by

$$\rho(t) = e^{\mathfrak{L}(t-t_0)}\rho(t_0), \tag{2.4.5}$$

where the *Liouville superoperator* is defined by

$$\mathfrak{L}(t)\rho = -i\ [\mathrm{H}_{\mathrm{tot}}(t), \rho(t)]\,.$$

If we want to obtain the evolution of the density operator for a system $\mathcal{A}$ excluding an environment $\mathcal{B}$ (as in Figure 2.1), we can make use of Equations (2.4.2) and (2.4.3). Since the total density matrix ρ evolves unitarily, that is,

$$\rho(t) = U(t, t_0)\rho(t_0)U^{\dagger}(t, t_0),$$

$$\rho_{\mathcal{A}}(t) = \mathrm{Tr}_{\mathcal{B}}\left(\rho(t)\right) \tag{2.4.6}$$

$$= \mathrm{Tr}_{\mathcal{B}}\left(U(t, t_0)\ \rho(t_0)\ U^{\dagger}(t, t_0)\right). \tag{2.4.7}$$

Similarly, the specific equation of motion can be worked out,

$$\frac{d}{dt}\rho_{\mathcal{A}}(t) = -i\ \mathrm{Tr}_{\mathcal{B}}\left[\mathrm{H}(t), \rho(t)\right].$$

Let $(|b_k\rangle)$ be an orthonormal basis for the environment $\mathcal{B}$. For example, let the initial state of the environment be the pure state

$$\rho_{\text{env}}(t_0) = |b_0\rangle\langle b_0|.$$

Then, Equation (2.4.7) can be formulated as

$$\begin{aligned}\rho_{\mathcal{A}} &= \sum_k \langle b_k|U(\rho \otimes |b_0\rangle\langle b_0|)U^\dagger|b_k\rangle \\ &= \sum_k \mathrm{B_k}\rho\mathrm{B_k^\dagger},\end{aligned}$$

where $\mathrm{B_k}$ are the **Kraus operators** that act on the state space of the principal system and are defined as follows,

$$\mathrm{B_k} \equiv \langle b_k|U|b_0\rangle. \tag{2.4.8}$$

They are not unique since there can be different collections of Kraus operators with respect to different orthonormal basis for the environment. However, Kraus operators always abide to the completeness equation,

$$\begin{aligned}\sum_k \mathrm{B_k}^\dagger\mathrm{B_k} &= \sum_k \langle b_0|U^\dagger|b_k\rangle\langle b_k|U|b_0\rangle \\ &= I.\end{aligned}$$

Based on Postulate 3, $\mathrm{B_k}$ can be interpreted as *measurement operators*. We shall use them to formulate the Open Quantum Walk in the forthcoming chapter where we shall also present other types of random walks.

Chapter 3

Random Walks

Randomness has been a topic of great concern throughout the history of mankind. It plays a central role both in experimental and theoretical aspects of physics. In this chapter, we shall look at the theoretical implication of randomness in classical and quantum walks as well as in their self-avoiding version. Finally, we shall introduce the Open Quantum Walk.

A **random walk** is a process in which an object translates from a starting point through a series of successive steps, each associated with a random choice. For instance, this choice can be determined by throwing a die. The outcome is random and depends on a probability. Figure 3.1 illustrates an example of a random walk. The Brownian motion is the root of the mathematical description of randomness brought forward by A. Einstein in 1905 [3] and M. Smoluchowski in 1906 [4].

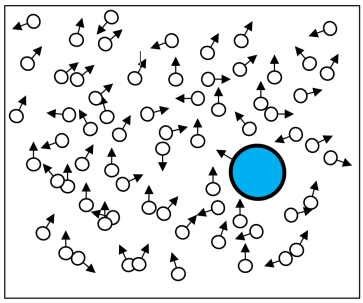

Figure 3.1: A blue dye particle colliding with water molecules, the arrows indicating their directions of motion.

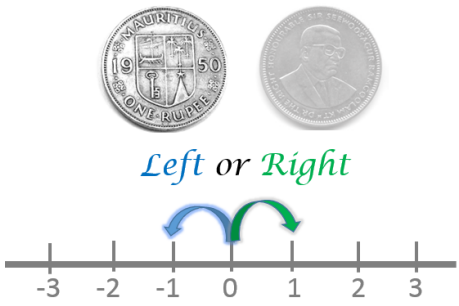

Figure 3.2: For a particle initially at the origin on a number line, a coin is used to determine the direction (left or right) of its first step. Its probability of moving in either direction is 0.5.

3.1 Classical Random Walks

Suppose that a particle is at an initial position zero on an integer axis (as shown in Figure 3.2). It can move its first step either to the right or to the left and this choice can be determined using a coin.

- For each step, the coin is tossed.
- If a head is obtained, the particle moves to the right; and if a tail is obtained, the particle moves to the left.
- After a number of steps, the distribution of the possible final position of the particle is plotted.

If the coin is *unbiased*, it is most likely that the particle will end up on the very starting point (See details in standard probability theory textbook such as [23]). Later, we shall compare the classical distribution arising from the above example with a quantum distribution.

Figure 3.3 is an example of a two-dimensional random walk. Starting from the origin, at each step, the walker has four choices of direction: up, down, right and left. We can relate the choices to the four cardinal points: North, South, East and West.

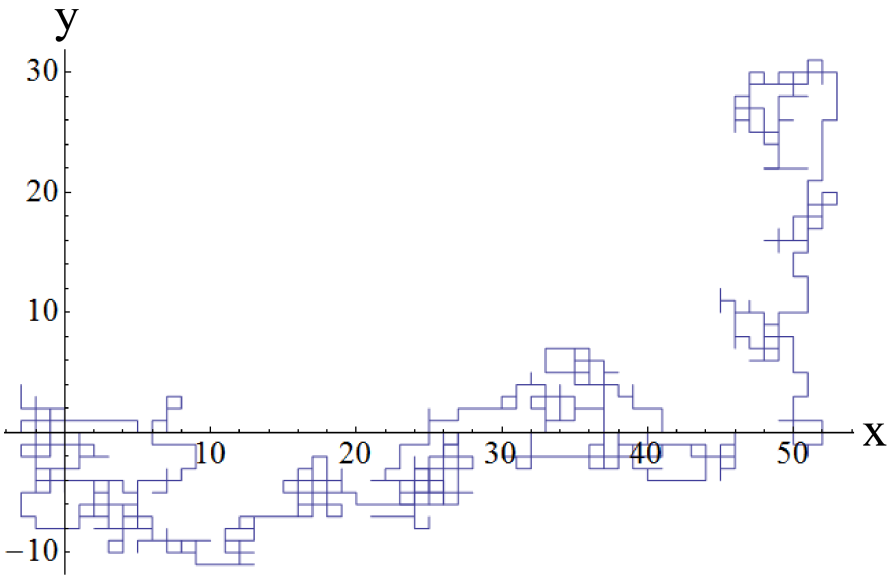

Figure 3.3: A trajectory of 1000 steps starting from the origin generated on Mathematica.

One can decipher from Figure 3.3 that many coordinates are visited more than once. In the next section, we shall see what happens when the coordinates cannot be revisited.

3.1.1 The Self-Avoiding Walk (SAW)

> *"The exact analysis of self-avoiding walks has stumped mathematicians for half a century; even counting the walks is a challenge."* [1]

Figure 3.4: Example of SAW: walking out of a maze (picture source: Wikipedia)

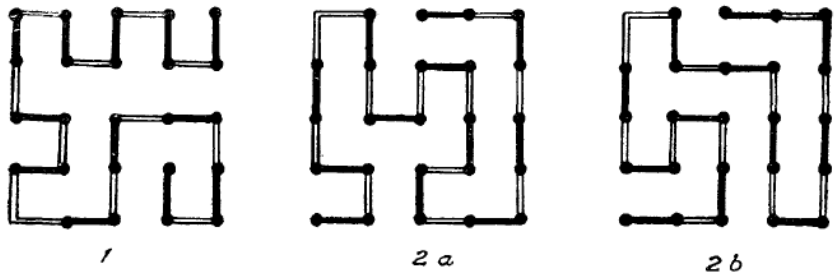

Figure 3.5: Random polymer chains: dimer represented by thick line; their bonds represented by double thin lines. (Picture source: [5])

A **Self-Avoiding Walk (SAW)** is a path on a lattice that does not visit the same site again. Figure 3.4 shows a common example of SAW. Some of the analytical questions about the SAW are unsolvable so far [24]. Yet, on a positive note, SAW has given rise to better understanding of stochastic differential equations [25] and probability theory [26]. Moreover, physicists and biologists make intensive use of it in modeling chemical processes. In fact, the first usage of SAW was to model a polymer in dilute solution as shown in Figure 3.5 [5, 6].

In the next section, we study SAWs that rely on random choices.

Implementation of the SAW

If the self-avoidance property is imposed on the one-dimensional walk described in section 3.1, the result will be a unidirectional walk either to the right or to the left, in other words, the simplest SAW. Whenever the variance will be measured, it will give zero. It is more meaningful to explore classical SAWs on a plane (two-dimension) or in space (three-dimension) [27]. Higher dimensions have been explored to determine the critical behaviour of SAW [28]. In the thesis, we focus on at most $2D$.

In figures 3.6 and 3.7, the walker cannot take a step further when it reaches the *red circle*. Therefore this is its ultimate *final position*. In the last chapter, we are going to compare the probability distribution of classical SAWs with that of non-unitary quantum walks. Before exploring non-unitary quantum dynamics, it is wise to review unitary ones.

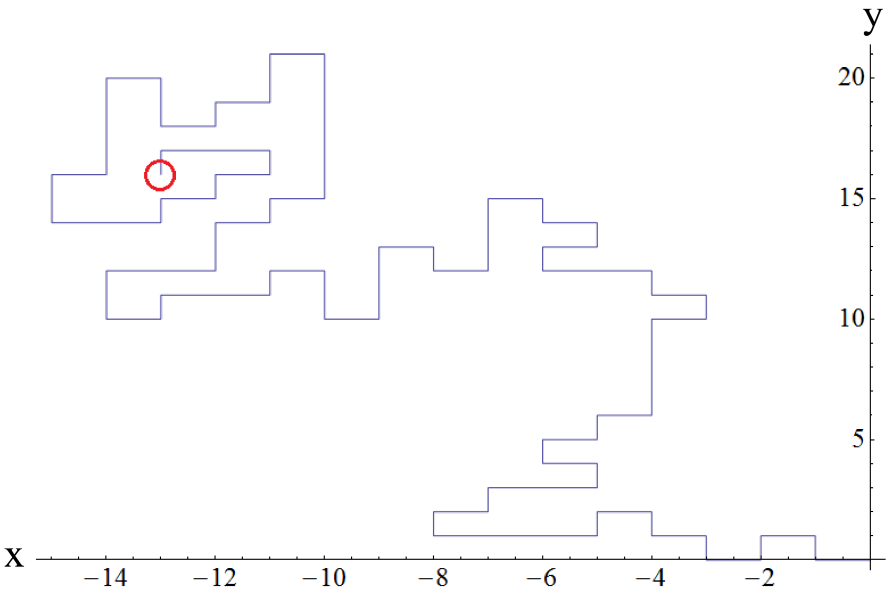

Figure 3.6: A self-avoiding trajectory of 99 steps: the particle starts from the origin and cannot move further when it reaches the red circle.

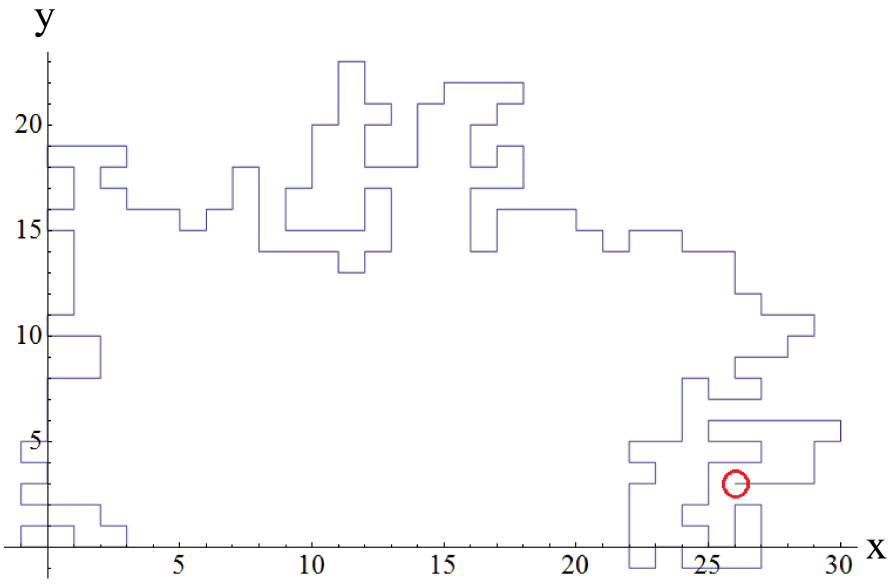

Figure 3.7: A self-avoiding trajectory of 207 steps: the particle starts from the origin and cannot move further when it reaches the red circle.

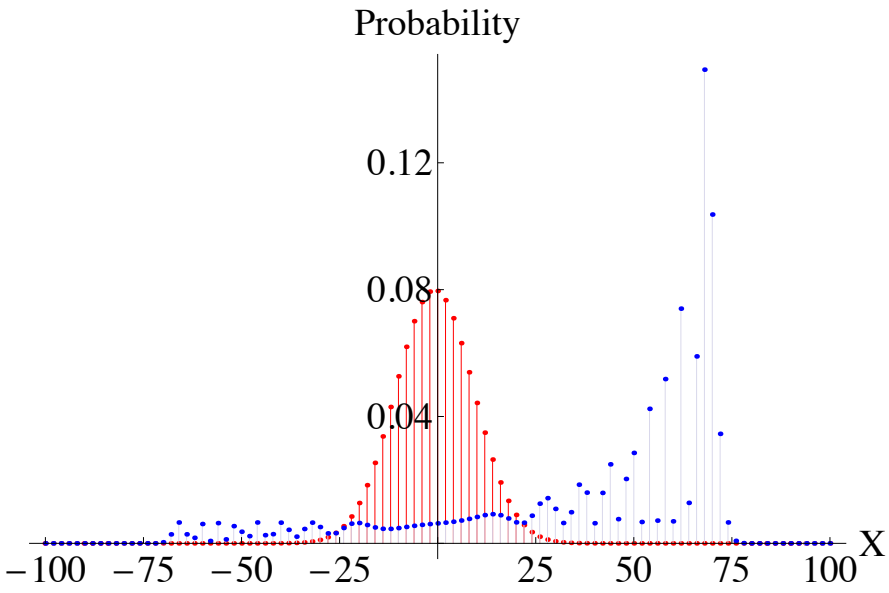

Figure 3.8: Probability distribution of $1D$ unitary quantum walk (in blue) using the Hadamard coin with initial condition $\{-\frac{1}{2}, \sqrt{3}/2\}$ and $1D$ classical random walk (in red) both starting at the origin.

3.2 Unitary Quantum Walks

The study of quantum walks started with Y. Aharonov, L. Davidovich and N. Zagury [29]. They demonstrated its application in quantum optics. In [30], its benefit to the field of quantum information science [31] is shown especially due to its algorithmic applications [32]. Several experiments [33, 34] and natural systems such as photosynthesis [35, 36] yield evidences that indeed a photon moves coherently in superposition through multiple pathways. This leads to interference effects which enable *quadratically* faster propagation when it comes to quantum walks [37]. On the $n-bit$ hypercube, quantum walks spread *exponentially* faster than classical walks [38].

What makes a quantum walk different from a classical one is the way the particle "walks" [39]. Their respective distribution is shown in Figure 3.8. The technicalities of the walk in one dimension is omitted. In the next section, we shall elaborate on the two-dimensional case which is more relevant to the subsequent parts of the chapter. Quantum walks can be realised experimentally [40] using the following methods:

1. Nuclear Magnetic Resonance
2. Cavity QED

3. Neutral atom traps

4. Quantum optics

We shall implement the unitary quantum walks on a cartesian plane based on the approach in [12] where the quantum SAWs were also analysed.

3.2.1 The mathematical formalism

Consider a two-dimensional lattice. Let $\mathcal{H}_p$ be the **position space** spanned by the basis $\{|x, y\rangle : x, y \in \mathbb{Z}\}$. Suppose that l stands for left, r for right, u for up and d for down. In vector notation,

$$|l\rangle = \begin{pmatrix} 1 \\ 0 \\ 0 \\ 0 \end{pmatrix}, |u\rangle = \begin{pmatrix} 0 \\ 1 \\ 0 \\ 0 \end{pmatrix}, |d\rangle = \begin{pmatrix} 0 \\ 0 \\ 1 \\ 0 \end{pmatrix}, |r\rangle = \begin{pmatrix} 0 \\ 0 \\ 0 \\ 1 \end{pmatrix}.$$

Then, let $\mathcal{H}_c$ be the **coin space** spanned by the basis $\{|l\rangle, |u\rangle, |d\rangle, |r\rangle\}$.

The *linear operators*, introduced in section 2.2, are leading elements of quantum walks. They can be devised with the help of the two bases stipulated above.

The **coin operator** is defined by

$$\mathrm{C} = \sum_{x,y \in \mathbb{Z}} |x, y\rangle\langle x, y| \otimes \mathrm{C}_0, \tag{3.2.1}$$

where C_0 is a unitary matrix. Therefore, C is *unitary*.

The four by four *Grover coin* is acquired by substituting C_0 with

$$\mathrm{C_G} = \frac{1}{2} \begin{pmatrix} -1 & 1 & 1 & 1 \\ 1 & -1 & 1 & 1 \\ 1 & 1 & -1 & 1 \\ 1 & 1 & 1 & -1 \end{pmatrix}. \tag{3.2.2}$$

It gives rise to the *Grover walk* which will be presented later on.

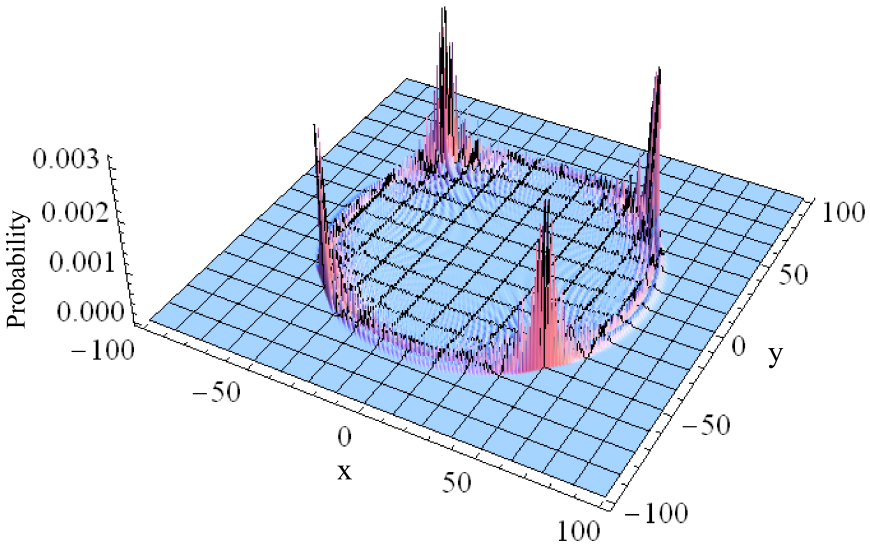

Figure 3.9: Grover walk starting from the origin with real initial state (3.2.7).

The operator responsible for the translation of the walker after the "tossing of the coin" is also *unitary*. It is called the **step operator** and is defined by

$$\begin{aligned} \mathrm{S} = \sum_{x,y\in\mathbb{Z}} (&|x+1,y\rangle\langle x,y| \otimes |r\rangle\langle r| + |x-1,y\rangle\langle x,y| \otimes |l\rangle\langle l| \\ &+|x,y+1\rangle\langle x,y| \otimes |u\rangle\langle u| + |x,y-1\rangle\langle x,y| \otimes |d\rangle\langle d|). \end{aligned} \tag{3.2.3}$$

Given an initial state of a particle located at the origin,

$$|\Psi_0\rangle = |0,0\rangle \otimes (\alpha|l\rangle + \beta|u\rangle + \gamma|d\rangle + \delta|r\rangle), \tag{3.2.4}$$

where $\alpha, \beta, \gamma, \delta \in \mathbb{C}$ such that

$$|\alpha|^2 + |\beta|^2 + |\gamma|^2 + |\delta|^2 = 1,$$

we can formulate the discrete evolution of the **unitary quantum walk** as follows,

$$|\Psi_t\rangle = (\mathrm{S.C})^t |\Psi_0\rangle, \tag{3.2.5}$$

where $|\Psi_t\rangle \in \mathcal{H}_p \otimes \mathcal{H}_c$, $t \in \{0,1,2,...\}$.

Furthermore, given that (X_t, Y_t) denotes the position (x,y) of the particle and $j \in \{l,u,d,r\}$, then the **probability distribution** of the particle is given at time t by

$$P(X_t, Y_t) = \langle\Psi_t| \left(|x,y\rangle\langle x,y|\right) |\Psi_t\rangle. \tag{3.2.6}$$

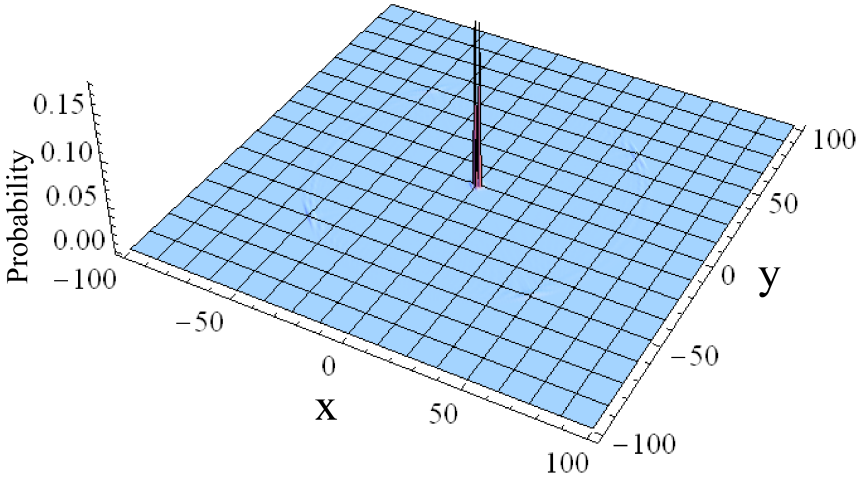

Figure 3.10: Grover walk starting from the origin with complex initial state (3.2.8).

A well-known example of a quantum walk is attributed to the *Grover search algorithm* [19]. One of the future aims of the formulation of the non-reversal OQW in this thesis could be to optimise this algorithm. Let us see how the probability distribution of this example varies with the initial state applied.

3.2.2 The Grover walk

We have already introduced the *Grover coin* in Equation (3.2.2). The step operator for all the unitary quantum walks that will be presented henceforth is the same as in Equation (3.2.3). Consider Equation (3.2.5) with the initial state,

$$|\Psi_0\rangle = \frac{1}{2}|0,0\rangle \otimes (|l\rangle - |u\rangle - |d\rangle + |r\rangle). \tag{3.2.7}$$

Then, the graph in Figure 3.9 is the probability distribution of the quantum walk after 100 steps.

Consider Equation (3.2.5) with a complex initial state:

$$|\Psi_0\rangle = \frac{1}{2}|0,0\rangle \otimes (|l\rangle + i|u\rangle + i|d\rangle - |r\rangle), \tag{3.2.8}$$

Then, the outcome is a **strongly localised distribution** as shown in Figure 3.10. Figure 3.10 is used as a reference to demonstrate self-avoidance property of other unitary quantum walks. In the next section, we review how this is done in [12] and [13].

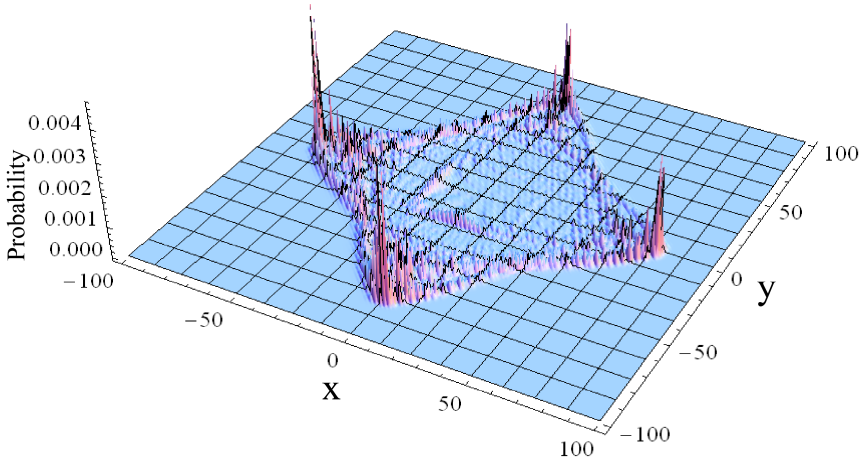

Figure 3.11: Probability distribution of 100-step non-reversal quantum walk starting from the origin with initial state (3.2.8).

3.3 Unitary Quantum Walks in Subspaces

By using the same complex initial state as for the Grover walk but varying the coin operator, three partially self-avoiding quantum walks are generated in *subspaces* of the *complete Hilbert space* [12]. In the **position space**, it is called **the non-reversal walk** and in the **coin space**, the **non-repeating walk**. The third one takes place in the union of the two subspaces.

3.3.1 Non-reversal quantum walks (in position space)

One way of perceiving the non-reversal walk is that it is halfway between a purely random walk and a Self-Avoiding Walk [1]. The walker cannot go back to its previous site. The non-reversal coin operator is defined by substituting the following unitary matrix into Equation (3.2.1).

$$\mathrm{C}^{\mathrm{rev}} = \frac{1}{\sqrt{3}} \begin{pmatrix} -1 & 1 & 1 & 0 \\ 1 & 1 & 0 & 1 \\ -1 & 0 & -1 & 1 \\ 0 & 1 & -1 & -1 \end{pmatrix}. \tag{3.3.1}$$

We use initial state (3.2.8) to produce the probability distribution in Figure 3.11. A wide square is observed. The number of distinctive peaks and their heights at the corners are affected by varying the initial condition on the walker [13].

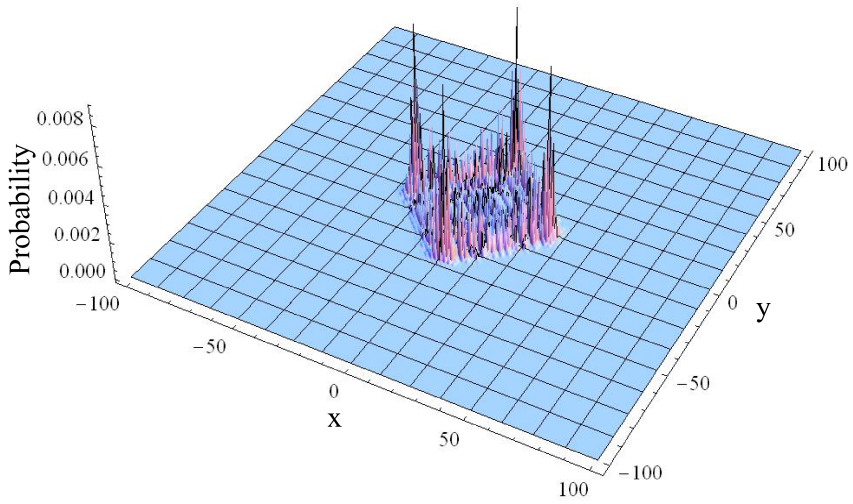

Figure 3.12: Probability distribution of 100-step non-repeating quantum walk starting from the origin with initial state (3.2.8).

3.3.2 Non-repeating quantum walks (in coin space)

In the non-repeating walk, a particle has to change direction at every step. The coin of this walk is obtained by permuting the non-reversal coin operator;

$$\mathrm{C}^{\mathrm{rep}} = \mathrm{C}^{\mathrm{rev}}.\begin{pmatrix} 0 & 0 & 0 & 1 \\ 0 & 0 & 1 & 0 \\ 0 & 1 & 0 & 0 \\ 1 & 0 & 0 & 0 \end{pmatrix}.$$

$$\text{Thus, } \mathrm{C}^{\mathrm{rep}} = \frac{1}{\sqrt{3}}\begin{pmatrix} 0 & 1 & 1 & -1 \\ 1 & 0 & 1 & 1 \\ 1 & -1 & 0 & -1 \\ -1 & -1 & 1 & 0 \end{pmatrix}.$$

The diagonal entries being zeros ensures that the walker does not move in the same direction in two successive steps. The corresponding distribution is displayed in Figure 3.12. A square is again observed. Here too, a variation in the initial condition on the walker affects the number of peaks and their size. In fact, the non-repeating quantum walk is interconnected to the non-reversal quantum walk. A more general form of the non-repeating coin operator has been given in [13],

$$\mathrm{C}^{\mathrm{rep}} = \begin{pmatrix} 0 & \lambda e^{i\alpha} & \gamma e^{i\beta} & f(\lambda,\gamma)e^{i\theta} \\ \lambda e^{-i(\phi+\delta+\alpha)} & 0 & -f(\lambda,\gamma)e^{i(\psi-\theta+\beta)} & \gamma e^{i\psi} \\ -\gamma e^{-i(\delta+\alpha+\psi)} & -f(\lambda,\gamma)e^{i(\phi-\theta+\alpha)} & 0 & \lambda e^{i\phi} \\ f(\lambda,\gamma)e^{i(\theta-\alpha-\psi-\phi-\beta)} & -\gamma e^{i(\delta+\alpha-\beta)} & \lambda e^{i\delta} & 0 \end{pmatrix},$$

where $0 \leq \gamma^2 + \lambda^2 \leq 1$ and $f(\lambda,\gamma) = \sqrt{1-(\gamma^2+\lambda^2)}$. The values of the real variables are available in [13].

3.3.3 Quantum walks in position and coin space

When the definitions of both the non-reversal and non-repeating quantum walks are combined, a distribution of quantum SAW in the union of position and coin space is obtained. The walker cannot step back where it has been before and it cannot move in the same direction as it did previously. The coin that fulfills these criteria is given by:

$$\mathrm{C}^{\mathrm{scp}} = \frac{1}{\sqrt{2}} \begin{pmatrix} 0 & -1 & 1 & 0 \\ 1 & 0 & 0 & -1 \\ 1 & 0 & 0 & 1 \\ 0 & 1 & 1 & 0 \end{pmatrix}. \tag{3.3.2}$$

The corresponding probability distribution is shown in Figure 3.13. It resembles that of the Grover walk with the real initial state (3.2.7).

So far, we were dealing with discrete quantum walks in a closed physical system. To conclude this section, it is worth mentioning that *continuous* quantum walks can also be modeled in a closed system [41]. In that case, the evolution of the walk does not require a coin. This could be another method of developing the self-avoiding adaptation of unitary quantum walks. Our next concern will be discrete quantum walks in an *open quantum system*.

3.4 Open Quantum Walks (OQW)

This section is the heart of the thesis. The model of the non-reversal Open Quantum Walk is attributed to the theory elucidated here.

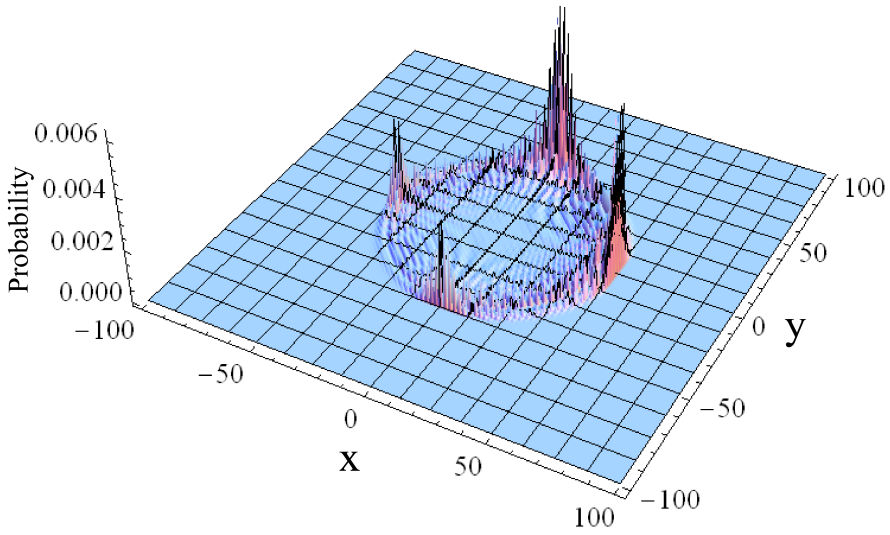

Figure 3.13: Probability distribution of 100-step quantum SAW, starting from the origin with initial state (3.2.8), using coin (3.3.2).

The **Open Quantum Walk** is formulated as classical Markov chain on graphs [42]. It is the quantum version of the classical random walk mentioned in the beginning of the chapter. It is vital to point out that *decoherence* plays a key role in such type of Markov chains. Although we will not elaborate on the aspect of decoherence here, one may choose to read further from [43].

3.4.1 The mathematical formalism

The mathematical formalism for the Open Quantum Walk has been detailed in [16]. Here, we adapt it to the two-dimensional version.

Let $\mathcal{V}$ be a set of coordinates on a cartesian plane. Then, $\mathcal{K} = \mathbb{C}^{\mathcal{V}}$ is the state space of a quantum system with as many basis vectors as the number of vertices in $\mathcal{V}$.

For every edge (connection between two coordinates), the bounded operator $B_{i,j}^{x,y} \in \mathcal{H}$ acts as a generalized quantum coin. It stands for the effect of translating from the coordinate (i, j) to the coordinate (x, y) as shown in Figure 3.14.

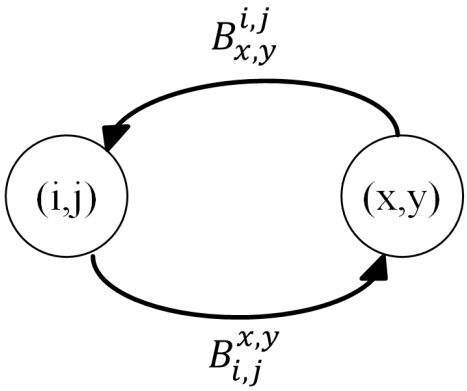

Figure 3.14: Translation between two arbitrarily adjacent coordinates (i, j) and (x, y).

In order for probability and positivity to be conserved, for each (i, j),

$$\sum_{(x,y)} B^{x,y\dagger}_{i,j} B^{x,y}_{i,j} = I. \tag{3.4.1}$$

Furthermore, given the structure of the density operator of the form,

$$\rho = \sum_{(x,y)} \rho_{x,y} \otimes |x, y\rangle\langle x, y|, \tag{3.4.2}$$

the condition that ρ is a state is realised by

$$\sum_{(x,y)} \mathrm{Tr}(\rho_{x,y}) = 1,$$

where each $\rho_{x,y}$ is not necessarily a density matrix on $\mathcal{H}$. Although $\rho_{x,y}$ is a positive and trace-class operator, its trace may not be 1.

For each $(i, j) \in \mathcal{V}$, a completely positive and trace preserving map on $\mathcal{H}$ of the density operator $\rho \in \mathbf{B}(\mathcal{H})$ can be defined as

$$M_{i,j}(\rho) = \sum_{(x,y)} B^{x,y}_{i,j} \rho B^{x,y\dagger}_{i,j}. \tag{3.4.3}$$

In order to "project" $M_{i,j}$ on the augmented space $\mathcal{H} \otimes \mathcal{K}$, the following extension is used,

$$M^{x,y}_{i,j} = B^{x,y}_{i,j} \otimes |x, y\rangle\langle i, j|. \tag{3.4.4}$$

Given that

$$\sum_{(x,y),(i,j)} M_{i,j}^{x,y\dagger} M_{i,j}^{x,y} = I,$$

a completely positive and trace preserving map can be defined on the total system, $\mathcal{H} \otimes \mathcal{K}$, as

$$\mathcal{M}(\rho) = \sum_{(x,y)} \sum_{(i,j)} M_{i,j}^{x,y} \rho M_{i,j}^{x,y\dagger}, \tag{3.4.5}$$

where $\rho \in \mathbf{B}(\mathcal{H} \otimes \mathcal{K})$. By iterating this map such that the structure of the density operator given in Equation (3.4.2) is conserved, the Open Quantum Walk (OQW) is produced. It can be restated as follows,

$$\mathcal{M}(\rho) = \sum_{(x,y)} \left(\sum_{(i,j)} B_{i,j}^{x,y} \rho_{i,j} B_{i,j}^{x,y\dagger} \right) \otimes |x,y\rangle\langle x,y|. \tag{3.4.6}$$

Given any initial state $\rho^{[0]}$ on $\mathcal{H} \otimes \mathcal{K}$, then all the states are of the form

$$\begin{aligned} \rho^{[n]} &= \mathcal{M}^n(\rho^{[0]}) \ \ \forall n \geq 1 \\ &= \sum_{(x,y)} \rho_{x,y}^{[n]} \otimes |x,y\rangle\langle x,y|, \\ \text{where } \rho_{x,y}^{[n+1]} &= \sum_{(i,j)} B_{i,j}^{x,y} \rho_{i,j}^{[n]} B_{i,j}^{x,y\dagger}. \end{aligned}$$

Moreover, the probability distribution, $P^{[n]}$ on $\mathcal{V}$, of the Open Quantum Walk at time n, $\forall n \geq 1$, is given by

$$P_{x,y}^{[n]} = \mathrm{Tr}(\rho_{x,y}^{[n]}), (x,y) \in \mathcal{V}. \tag{3.4.7}$$

3.4.2 The "coins"

Assuming four directions of motion of a particle on a plane, a quantum coin is required to govern each of them. If the directions are related to the cardinal points North, South, East, West, then, the coins are given by

$$\begin{aligned} E &= B_{i,j}^{i+1,j} \text{ (East)}, \\ W &= B_{i,j}^{i-1,j} \text{ (West)}, \\ N &= B_{i,j}^{i,j+1} \text{ (North)}, \\ S &= B_{i,j}^{i,j-1} \text{ (South)}. \end{aligned}$$

The corresponding condition responsible for the conservation of probability and positivity in the Open Quantum Walk formalism is stated as follows.

$$E^\dagger E + W^\dagger W + N^\dagger N + S^\dagger S = I. \tag{3.4.8}$$

Two of the ways of procuring the quantum coins are presented below.

Method 1

We take any four by four unitary matrix. Using each of its row, we construct new four by four matrices as in Example 3.4.1.

Example 3.4.1.
Consider the unitary matrix (3.3.1). Then, the four required matrices are:

$$N = \frac{1}{\sqrt{3}} \begin{pmatrix} -1 & 1 & 1 & 0 \\ 0 & 0 & 0 & 0 \\ 0 & 0 & 0 & 0 \\ 0 & 0 & 0 & 0 \end{pmatrix},$$

$$E = \frac{1}{\sqrt{3}} \begin{pmatrix} 0 & 0 & 0 & 0 \\ 1 & 1 & 0 & 1 \\ 0 & 0 & 0 & 0 \\ 0 & 0 & 0 & 0 \end{pmatrix},$$

$$W = \frac{1}{\sqrt{3}} \begin{pmatrix} 0 & 0 & 0 & 0 \\ 0 & 0 & 0 & 0 \\ -1 & 0 & -1 & 1 \\ 0 & 0 & 0 & 0 \end{pmatrix},$$

$$S = \frac{1}{\sqrt{3}} \begin{pmatrix} 0 & 0 & 0 & 0 \\ 0 & 0 & 0 & 0 \\ 0 & 0 & 0 & 0 \\ 0 & 1 & -1 & -1 \end{pmatrix}.$$

One can verify that indeed condition (3.4.8) is respected, that is,

$$E^\dagger E + W^\dagger W + N^\dagger N + S^\dagger S = I.$$

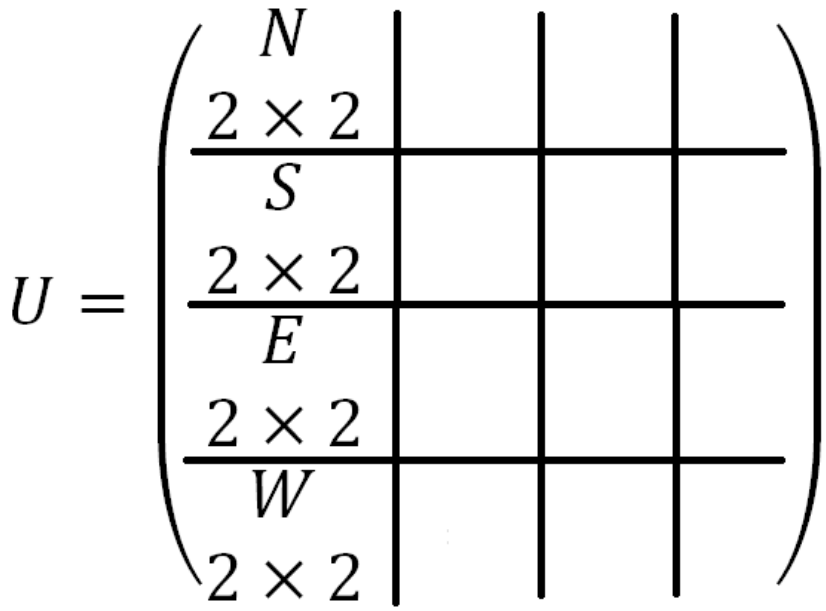

Figure 3.15: An illustration of how to extract four Kraus matrices from an 8 by 8 unitary matrix.

Method 2

For a two-dimensional OQW, the coins can be n by n Kraus operators provided the initial density state is also n by n. However, we restrict the description below to the simplest case of two by two matrices which we shall use for the simulation of most of our walks. The Python code for the following method is given in Appendix A.1. It generates complex matrices unlike the previous method.

Step 1 Generate a random 8 by 8 *unitary* matrix, U.

Step 2 Considering the first two columns of U, construct the 4 required matrices as follows. Obtain:

- N using the first 2 rows,
- S using the second 2 rows,
- E using the third 2 rows,
- W using the last 2 rows.

Figure 3.15 shows the position of the four matrices, N, S, E and W in an 8 by 8 unitary matrix.

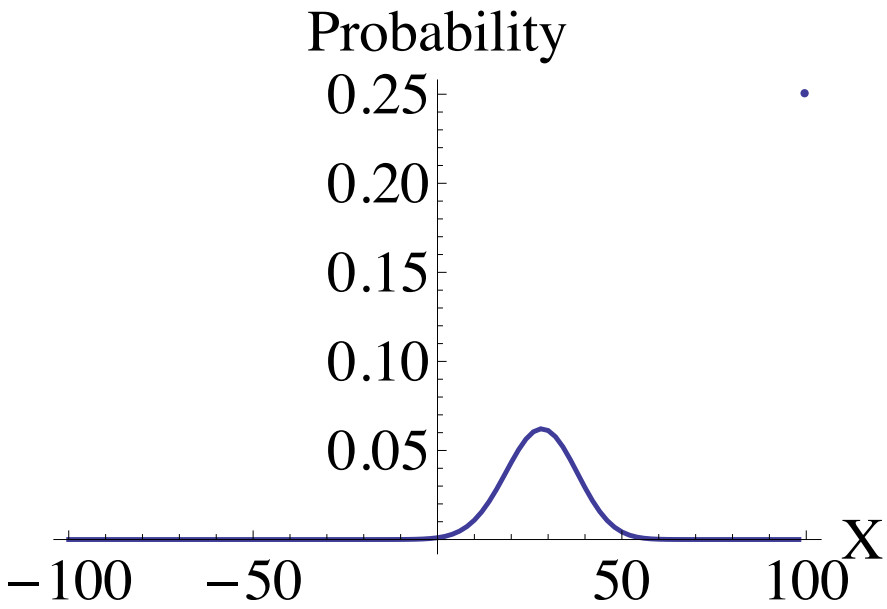

Figure 3.16: Probability distribution after 100 steps of $1D$ OQW starting from the origin with initial density state (3.4.9) and using the coins (3.4.10) and (3.4.11). Besides the Gaussian peak, a soliton can be observed with very high probability.

3.4.3 The probability distribution

As an example, a one-dimensional Open Quantum Walk on the set of integers, $\mathbb{Z}$, is considered. Let the initial density state be given by

$$\rho^{[0]} = \frac{1}{4}\begin{pmatrix} 1 & -\sqrt{3} \\ -\sqrt{3} & 3 \end{pmatrix}. \tag{3.4.9}$$

Then, Figure 3.16 illustrates the probability distribution of the OQW after 100 steps arising from the following bounded operators:

$$B = \begin{pmatrix} 1 & 0 \\ 0 & \frac{4}{5} \end{pmatrix}, \tag{3.4.10}$$

$$C = \begin{pmatrix} 0 & 0 \\ 0 & \frac{3}{5} \end{pmatrix}. \tag{3.4.11}$$

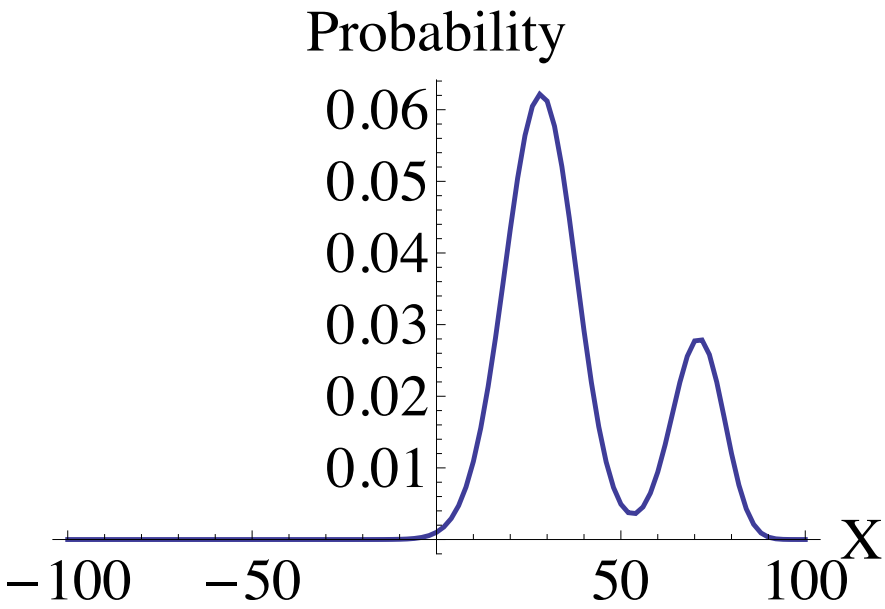

Figure 3.17: Probability distribution of $1D$ OQW with 2 Gaussian peaks. The walk starts from the origin with initial density state (3.4.9) and using the coins (3.4.12) and (3.4.13).

Suppose that the following coins are used instead in the above example.

$$B = \begin{pmatrix} \frac{12}{13} & 0 \\ 0 & \frac{4}{5} \end{pmatrix}, \tag{3.4.12}$$

$$C = \begin{pmatrix} \frac{5}{13} & 0 \\ 0 & \frac{3}{5} \end{pmatrix}. \tag{3.4.13}$$

Then, the probability distribution of the walk is given in Figure 3.17.

If we apply Method 1 (described earlier) to the Hadamard matrix in Equation (2.2.1), we obtain the following "coins":

$$B = \frac{1}{\sqrt{2}} \begin{pmatrix} 1 & 1 \\ 0 & 0 \end{pmatrix}, \tag{3.4.14}$$

$$C = \frac{1}{\sqrt{2}} \begin{pmatrix} 0 & 0 \\ 1 & -1 \end{pmatrix}. \tag{3.4.15}$$

The corresponding OQW distribution after 100 steps is given in Figure 3.18. It resembles the classical distribution that was illustrated in Figure 3.8.

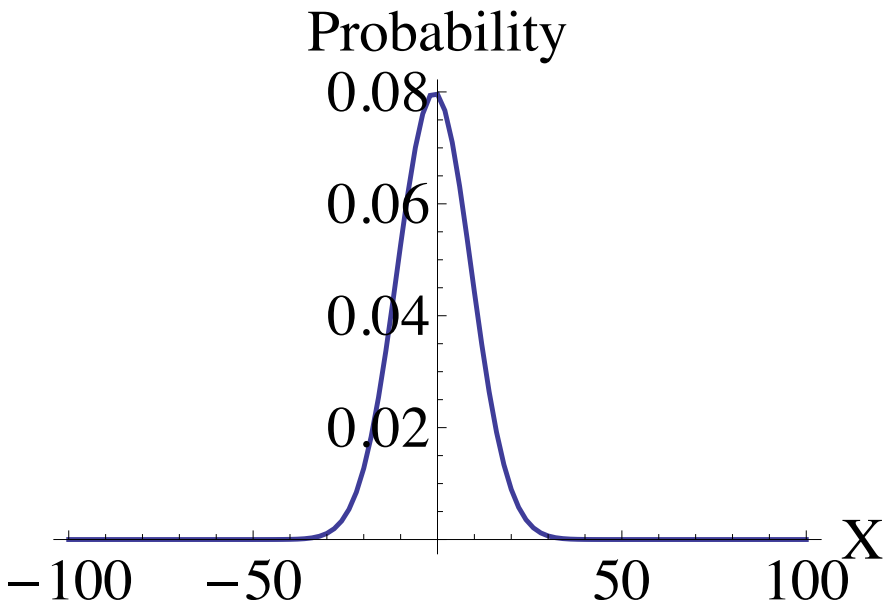

Figure 3.18: Probability distribution of "Hadamard" OQW starting from the origin with initial state (3.4.9) and bounded operators (3.4.14) & (3.4.15).

The same procedure can be done for $2D$ OQW. Let the initial density state be

$$\rho^{[0]} = \frac{1}{4}\begin{pmatrix} 1 & 0 & 0 & 0 \\ 0 & 1 & 1 & 0 \\ 0 & 1 & 1 & 0 \\ 0 & 0 & 0 & 1 \end{pmatrix}. \tag{3.4.16}$$

If we apply Method 1 to the Grover coin, the corresponding distribution is given in Figure 3.19. If Method 2 is used instead with initial state (3.4.9), then the Gaussian distribution in Figure 3.20 is obtained.

On the experimental side, a plausible quantum optical realisation of Open Quantum Walks was proposed recently [44]. In the next chapter, the OQW with non-reversal property will be studied.

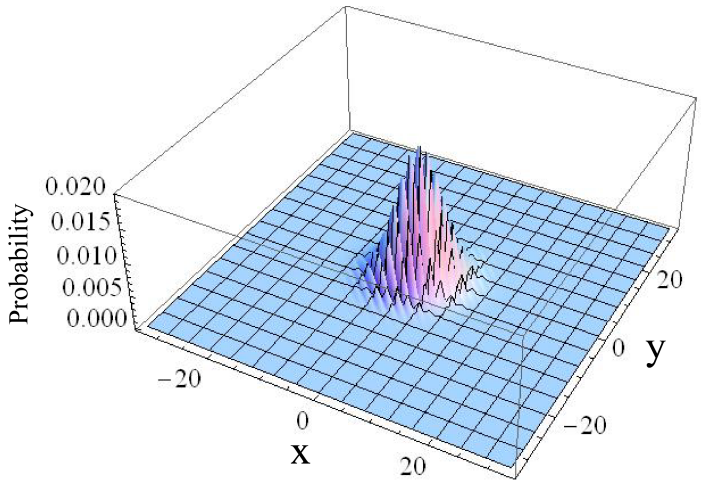

Figure 3.19: Probability distribution of "Grover" OQW starting from the origin with initial state (3.4.16). The 4 bounded operators are obtained by applying Method 1 to the Grover coin.

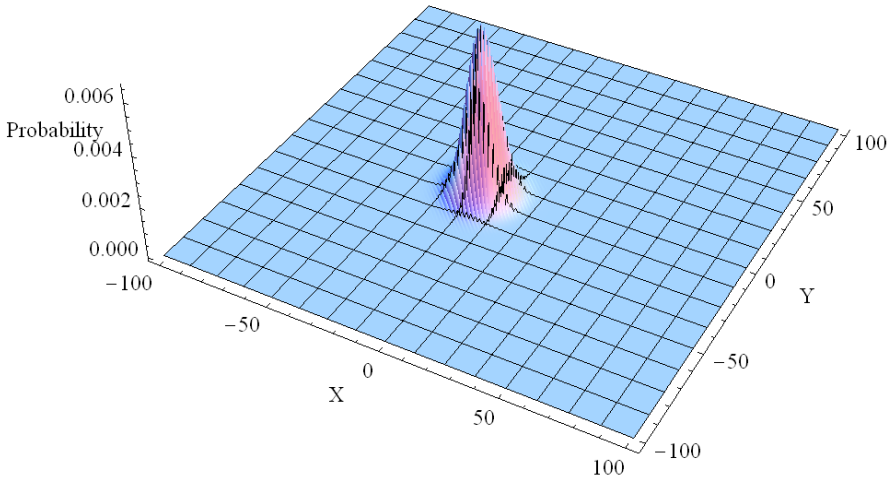

Figure 3.20: Probability distribution of OQW starting from the origin with initial state (3.4.9). The 4 bounded operators are obtained from a randomly generated unitary matrix (Method 2).

Chapter 4

Non-reversal Open Quantum Walk

"Quantum physics thus reveals a basic oneness of the universe."

Erwin Schrödinger (1887 − 1961)

In the last chapter, a new model of Open Quantum Walk with non-reversal property is suggested. It is based on the principle of quantum trajectories which is introduced in the first section of the chapter. The non-reversal OQW is presented in one dimension with emphasis on the memory structure. The model is then extended to two dimension and its statistics is analysed with a possible application in the field of polymer physics.

Most parts of this chapter will be the contents of the manuscript [45],
Goolam Hossen, Y.H., Sinayskiy, I. and Petruccione, F., 2015. Non-reversal Open Quantum Walks. in preparation.

4.1 Quantum Trajectories

It is known that the behaviour of a particle in a quantum system is different from the classical world since it tends to move in superposition. The paths of the particle are called **quantum trajectories**. However, if the position of the particle is measured, its wavefunction collapses such that the particle appears to have moved only through one trajectory. When dealing with an open quantum system, a quantum trajectory can be "observed" without destroying the state of the particle. The technique is explained with the help of the OQW [16].

Given that a particle on a line with an initial state $\rho^{[0]}$, is mapped from a site (i,j) to a site (x,y) by $\mathcal{M}$, then, the partial random state of the particle with respect to its new position is given by

$$\rho^{[1]}_{x,y} \otimes |x,y\rangle\langle x,y| = B^{x,y}_{i,j}\rho^{[0]}_{i,j}B^{x,y\dagger}_{i,j} \otimes |x,y\rangle\langle x,y|,$$

where $B^{x,y}_{i,j}$ are the transition operators. Given that the position is measured, then, the new density state is given by

$$\rho^{[1]} = \frac{1}{P_{x,y}} B^{x,y}_{i,j}\rho^{[0]}B^{x,y\dagger}_{i,j} \otimes |x,y\rangle\langle x,y|,$$

where the probability to move to that position is

$$P_{x,y} = \mathrm{Tr}(B^{x,y}_{i,j}\rho^{[0]}B^{x,y\dagger}_{i,j}).$$

If the above mapping and measurement procedures are iterated, a non-homogenous Markov chain $(\rho^{[n]})$ is obtained with expectation value,

$$\mathbb{E}[\rho^{[n+1]}|\rho^{[n]} = \rho^{[0]}] = \mathcal{M}(\rho^{[0]}).$$

Hence, the Markov chain describes the quantum trajectory of the Open Quantum Walk.

Quantum trajectories are believed to decrease the cost of simulations of open systems [46]. Basically, suppose that the density matrix describing the system is of size $m \times m$. Then, only m entries of the reduced system needs to be determined for a single trajectory. Subsequently, many such trajectories are simulated and their average gives the solution of the master equation. Numerically, the method is cheaper. Later, it will be used to generate the probability distribution of the walks.

4.2 The Non-reversal OQW in 1D

It was mentioned in the previous chapter that the classical SAW on a line is unidirectional. The particle would keep going either to the right or to the left of its starting point. However, the condition of the walker can be adjusted so that it can either move to a previously unoccupied position or stay at the same site. Then, the term "step" does not necessarily mean moving. Rather, it refers to time-step. In this section, we formulate the quantum version of this more interesting model which is known as the **non-reversal walk**.

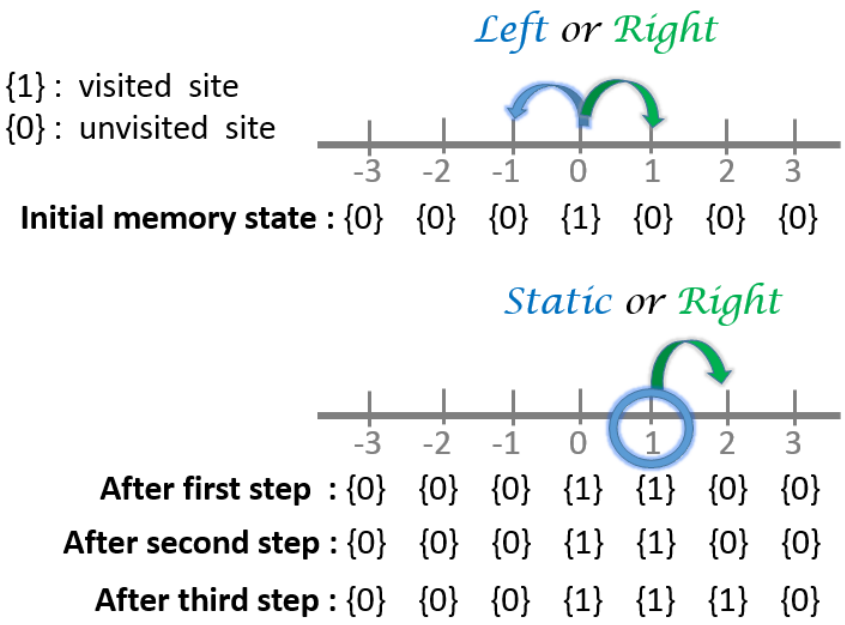

Figure 4.1: Memory update for $1D$ non-reversal OQW given that the walker starts from the origin, moves to the right in the first time-step, stays static in the second time-step and moves again to the right in the third time-step.

In the formalism of OQW, measurement of the position of the walker at any instant does not destroy the dynamics of the system unlike the case of unitary quantum walks. The reason is that the internal state of the walker, $\rho_{x,y}^{[n]}$, is independent of its position, $|x,y\rangle\langle x,y|$, at any time-step. This can be clearly seen from the definition of the density state,

$$\rho^{[n]} = \sum_{(x,y)} \rho_{x,y}^{[n]} \otimes |x,y\rangle\langle x,y| \quad \forall n \geq 1. \tag{4.2.1}$$

Hence, the non-reversal OQW can be formulated more reliably unlike the non-reversal unitary quantum walk in [13].

4.2.1 The need for memory

In order to ensure that the particle does not go back to a site where it has been before, a memory system is required. A permanent memory introduces decoherence in the system (appropriate for non-unitary dynamics). In our model, the memory system is associated with the line rather than with the state of the walker as in [47]. Initially, the memory state at each site is zero, except for the starting position (which is usually the origin as shown in Figure 4.1). When a particular site is visited, its memory state is altered to one.

4.2.2 Implementation of the walk

Consider a particle on the origin of a line with initial density state, $\rho^{[0]}$. Let B and C be two quantum coins associated with the particle's initial movement to the right and to the left respectively. The bounded operators obey the following condition of positivity and probability:

$$B^\dagger B + C^\dagger C = I. \tag{4.2.2}$$

Given that the direction is randomly chosen and suppose that the first step of the particle is to the right, then, its new state is given by

$$\rho_1^{[1]} = B_0^1 \rho_0^{[0]} B_0^{1\dagger}. \tag{4.2.3}$$

The position of the particle and the memory system are updated as shown in Figure 4.1. In the following "steps", the particle can either move to the right again or stay on the same spot. The role of the quantum coin B remains the same while coin C will henceforth be used to update the state of the particle when it does not move. For instance, assume that in the second "step", the particle stays on the same site. Then, its state is updated as follows,

$$\rho_1^{[2]} = C_1^1 \rho_1^{[1]} C_1^{1\dagger}. \tag{4.2.4}$$

A third update of the state is shown assuming that this time the particle moves to the right:

$$\rho_2^{[3]} = B_1^2 \rho_1^{[2]} B_1^{2\dagger}. \tag{4.2.5}$$

Figure 4.1 illustrates how the memory associated with the line is altered for these 3 "steps".

4.2.3 The probability distribution

The spread of the non-reversal OQW is investigated using the concept of averaging over many quantum trajectories. The "walk" is iterated at least 10 000 times on a finite number line (-100 to 100). After each process, the final position of the walker is recorded. Let it be x. Subsequently, the probability distribution of x is plotted.

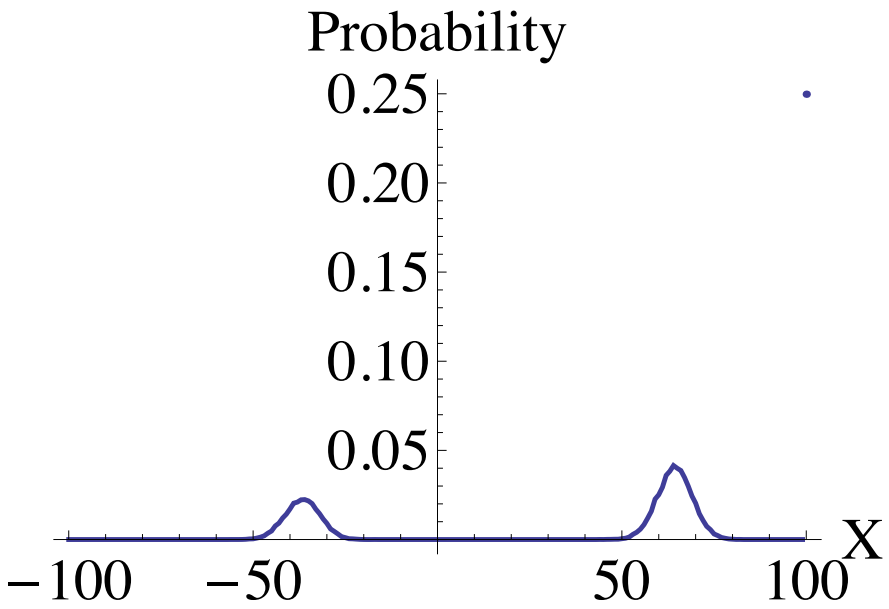

Figure 4.2: Probability distribution of the final positions x of non-reversal quantum trajectories on a line that start from the origin with initial density state (3.4.9) using the coins (3.4.10) and (3.4.11). 50000 iterations (instead of 10000) were carried out to obtain refined peaks.. A soliton can be observed on the top right.

As an example, consider a particle on the origin with initial density state (3.4.9) and let the pair of bounded operators be (3.4.10) and (3.4.11). Then, the distribution after 100 "steps" is illustrated in Figure 4.2. An interesting observation is the two small Gaussian peaks. If their probability values are added, the value of the single peak of the corresponding ordinary OQW in Figure 3.16 is obtained. This clearly demonstrates a diffusion on both sides of the origin due to the non-reversal property of the new OQW. Furthermore, the soliton, which was in Figure 3.16, also appears in Figure 4.2 with the same largest probability 0.25. This means that in most of the trajectories generated, the walker moved to the right in every step from the origin to the site $x = 100$.

Consider another example of non-reversal OQW using the same initial density state (3.4.9) but the different bounded operators given by (3.4.12) and (3.4.13). The distribution consists of four Gaussian peaks as shown in Figure 4.3. When contrasted with the double Gaussian OQW of Figure 3.17, the spread due to the unidirectional nature of the non-reversal walk is evident. Moreover, no soliton is produced in Figure 4.3. Hence, the non-reversal OQW follows the statement in [48] that soliton occurrence depends on the pair of transition operators used.

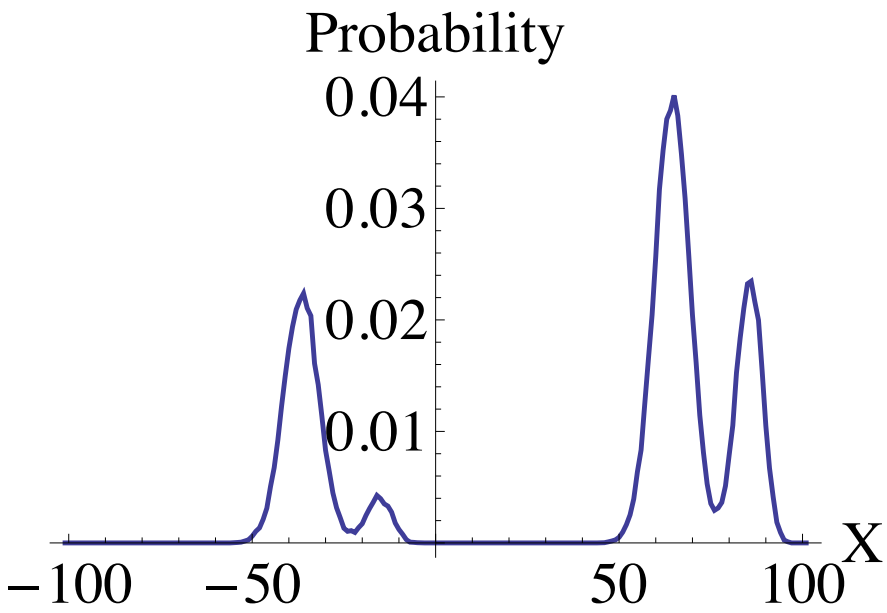

Figure 4.3: Probability distribution of the final position x of a walker given that it starts from the origin with initial density state (3.4.9) and the two coins used are (3.4.12) and (3.4.13). 100000 iterations (instead of 10000) were carried out to obtain refined peaks.

4.3 The Non-reversal OQW in 2D

On a plane, the directions of motion of a particle can be related to the cardinal points North (N), South (S), East (E), West (W). Let the choices of direction be governed by the following quantum coins,

$$\begin{aligned} E &= B_{i,j}^{i+1,j} \text{ (East)}, \\ W &= B_{i,j}^{i-1,j} \text{ (West)}, \\ N &= B_{i,j}^{i,j+1} \text{ (North)}, \\ S &= B_{i,j}^{i,j-1} \text{ (South)}. \end{aligned}$$

Then, the condition responsible for the conservation of probability and positivity in the formalism of the Open Quantum Walk is given by

$$E^\dagger E + W^\dagger W + N^\dagger N + S^\dagger S = I. \tag{4.3.1}$$

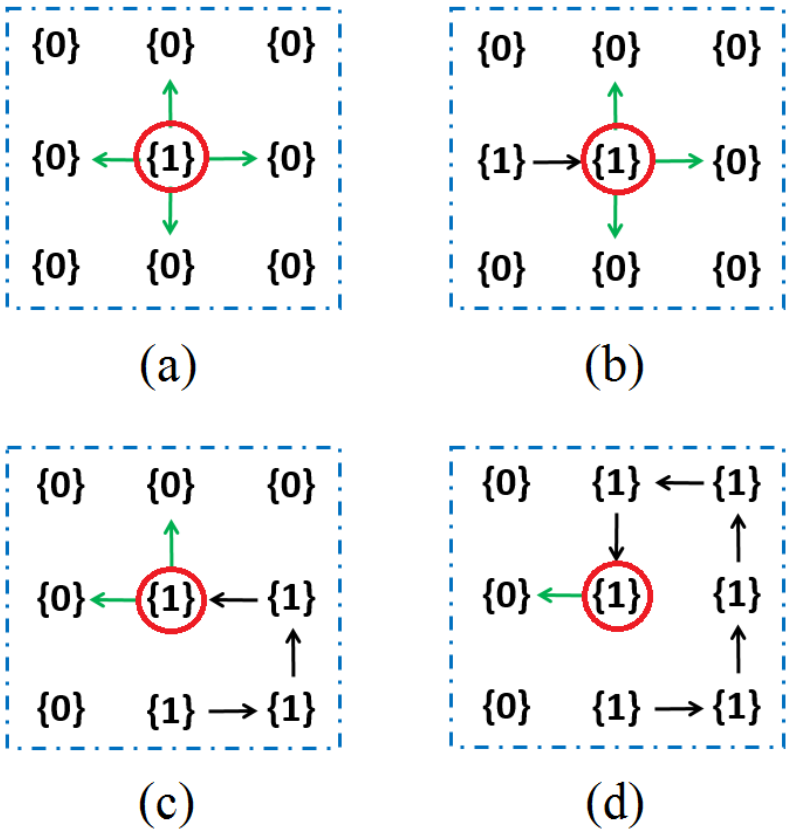

Figure 4.4: (a) to (d) are the 4 situations of a particle in a SAW. The red circle represents the current position of the particle. The green arrows indicate the possibilities of the next move and the black arrows show the few previous movements. (a) In the first step, the particle has the possibility of moving in four directions. (b) In the second and third steps, the walker can choose between three directions. (c) From the fourth step onwards, the number of choices depends on the previous moves of the walker. In some cases, the particle has two choices. (d) After the fifth step, the particle may have only one choice of direction.

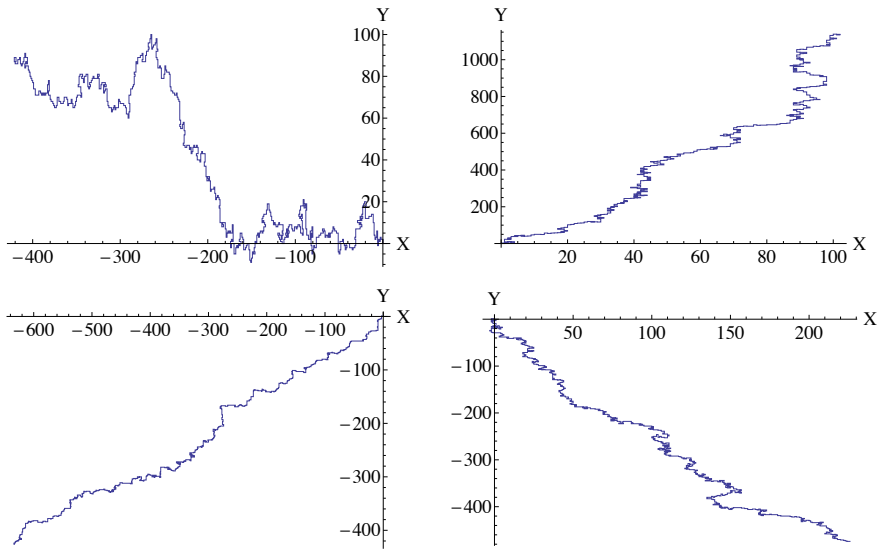

Figure 4.5: Non-reversal quantum trajectories of a particle initially at the origin that moves 2000 steps on a lattice of size 4001 by 4001. Different sets of quantum coins are used for each trajectory.

Why Not self-avoiding?

Figure 4.4 demonstrates the four different situations of a particle throughout a Self-Avoiding Walk (SAW) as well as the corresponding partial structures of the memory associated with the lattice. For the first step, the particle has four choices of direction. However, for all subsequent steps, it has less than four choices. In these situations, Equation (4.3.1) does not hold anymore. In order to overcome this problem, the principle of the non-reversal OQW in 1D is adapted. If the walker cannot move in the chosen direction, it stays on the same spot and its state is updated using the coin operator corresponding to the chosen direction. This was illustrated in Equation (4.2.4). As a result, the Open Quantum Walk cannot be completely self-avoiding. Thus, it is called the **non-reversal Open Quantum Walk**.

4.3.1 Implementation of the walk

Consider a particle on the origin of a plane with the initial density state given in Equation (3.4.9). Figure 4.5 shows some examples of non-reversal trajectories obtained using different sets of quantum coins. The coins are generated on Python as explained in Section 3.4.2. Interestingly, the simulated trajectories resemble closely real linear polymer structures as illustrated in Figure 4.6.

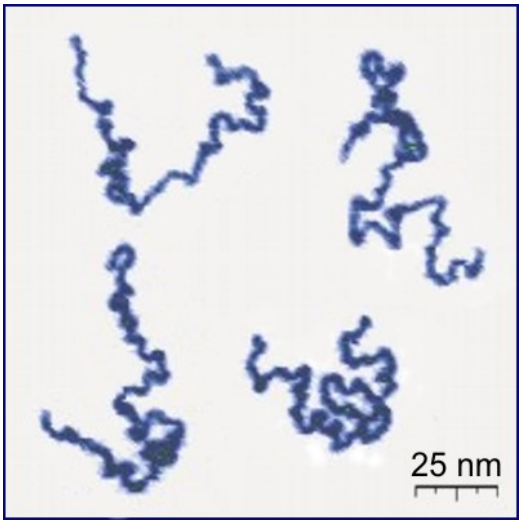

Figure 4.6: Appearance of real linear polymer chains as recorded using an atomic force microscope on a surface, under liquid medium (Ref. [49]).

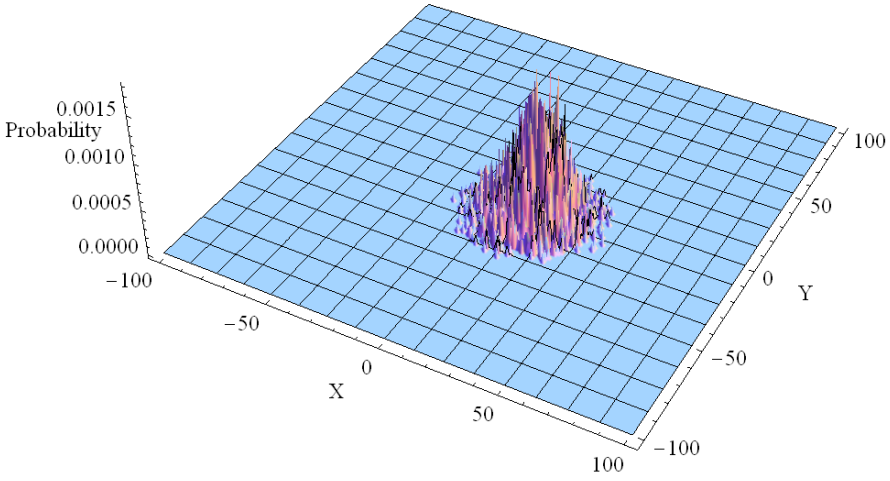

Figure 4.7: Probability distribution of non-reversal OQW after 100 steps starting from the origin with initial density state (3.4.9). The coins used are obtained from a randomly generated unitary matrix. The highest peak is at $(19, -18)$.

4.3.2 The probability distribution

We have seen earlier that averaging over many quantum trajectories helps in analysing the spread of the non-reversal OQW in 1D. The same principle is applied in 2D. At least 10000 trajectories similar to one of the examples in Figure 4.5 are generated and the final position (x, y) for each of them is recorded after 100 steps. It is worth pointing out that the same set of quantum coins is used for the 10000 trajectories. Then, the probability distribution of the final positions is plotted as shown in Figure 4.7.

4.3.3 Statistical analysis

Results for non-reversal OQW

From Figure 4.5, one can deduce that the direction of the trajectory of the particle varies with the set of coins used. At this stage, we ignore the detailed structure of the trajectory and focus more on its end-to-end distance. Therefore, probability distributions as in Figure 4.7 are of great help. In particular, the point at which the highest peak occurs is of interest. By using a large sample of quantum coins (10000 randomly generated unitary matrices, each giving one set of four coins), such points are recorded after a specific number of steps (see Figure 4.8).

Our earlier deduction from Figure 4.5 becomes more obvious when looking at Figure 4.8. Indeed, the trajectories can end in any of the four quadrants depending on which set of quantum coins was used. This reveals an interesting property of the non-reversal OQW that opens doors to further research. The direction of the spread can be tuned using specific Kraus operators.

The distance between the origin and any of the end points in Figure 4.8 is given by the norm of the respective coordinate. Each of these distances is called the radius, r, for the total number of steps. For instance, from Figure 4.7, when the norm of $(19, -18)$ is calculated, the value of the radius for 100 steps is 26.2. In the case of larger number of steps ($N = 400$), radii for intermediate number of steps ($N = 50, 100, 150, 200, 250, 300, 350$) are also recorded as shown in Figure 4.9. Their mean values and the standard deviation are given in Table 4.1. These values can be used to obtain the equation of the line of best fit in Figure 4.9. Else, one can simply use the function `LinearModelFit` available in Mathematica to obtain the equation,

$$r = 7.23682 + 0.218773N. \tag{4.3.2}$$

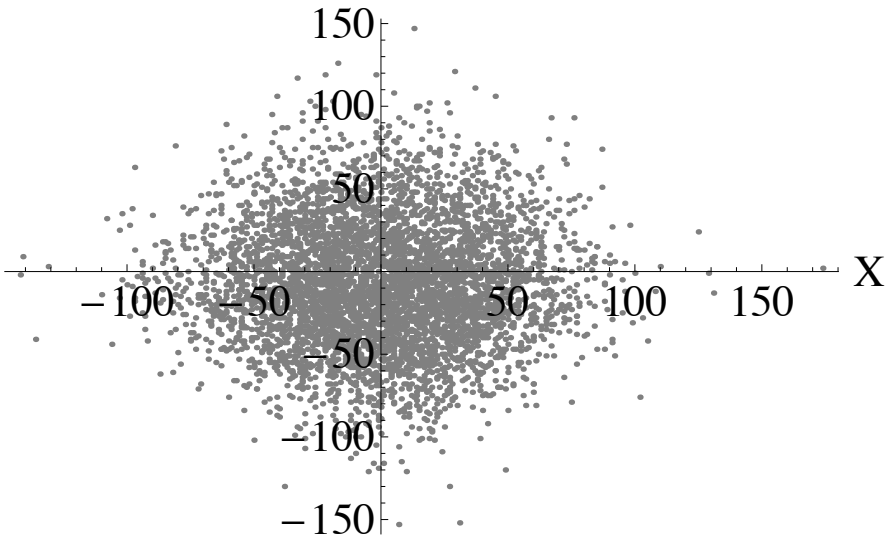

Figure 4.8: Most probable final positions of non-reversal quantum trajectories after 200 steps. Each end point depends on the quantum coins used to propagate the walk from the origin.

N	mean	standard deviation
50	18.486	08.245
100	29.982	13.941
150	40.575	19.213
200	51.108	24.701
250	60.803	29.487
300	72.100	34.623
350	83.296	39.527
400	96.057	44.293

Table 4.1: Mean values and standard deviation of the radii of the spread of non-reversal OQW for different number of steps, N.

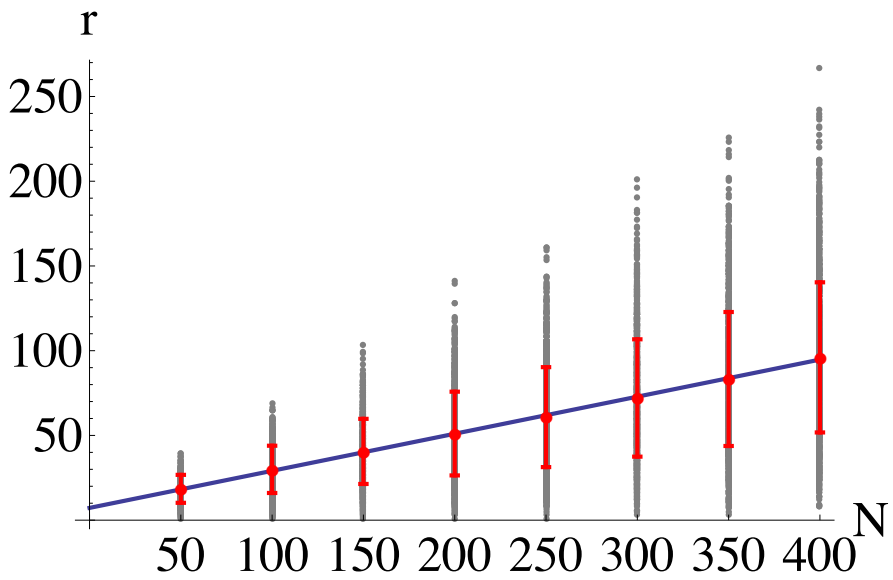

Figure 4.9: Distribution of the radii, r, of 10000 different spreads of non-reversal OQWs each arising from 10000 trajectories with number of steps, $N = 50$ to $N = 400$. The graph also illustrates the corresponding error bars for specific number of steps as well as the line of best fit determined by the mean values of r for the different N.

Results for OQW

With each of the randomly generated unitary matrix used for the non-reversal OQW, distributions of OQW for the different values of N are also produced from the resulting bounded operators and using the same initial density state given by Equation (3.4.9). In this case, the radius, r, refers to the distance between the origin and the point at which the Gaussian peak occurs. The values of the radii are plotted in Figure 4.10 for the number of steps, $N = 50$ to $N = 400$. Table 4.2 gives the mean values of the radii of the spreads of OQW for the specific number of steps. Using the the function `LinearModelFit` in Mathematica, the equation of the line of best fit is given by

$$r = 10.8911 + 0.218787N.$$

Although the line of best fit in Figure 4.10 tends to resemble the one in Figure 4.9 due to similar gradient values, their vertical intercepts are distinctly different. However, these graphs do not allow us to properly appreciate the difference between OQWs and their non-reversal versions but rather may mislead us to think that they are same. To clarify this ambiguity, we repeat the analysis for larger number of steps.

N	mean	standard deviation
50	19.205	08.355
100	32.684	14.938
150	44.492	21.090
200	54.959	27.224
250	65.850	32.803
300	76.426	38.619
350	86.951	44.919
400	98.577	50.888

Table 4.2: Mean values and standard deviation of the radii of the spread of OQW for different number of steps, N.

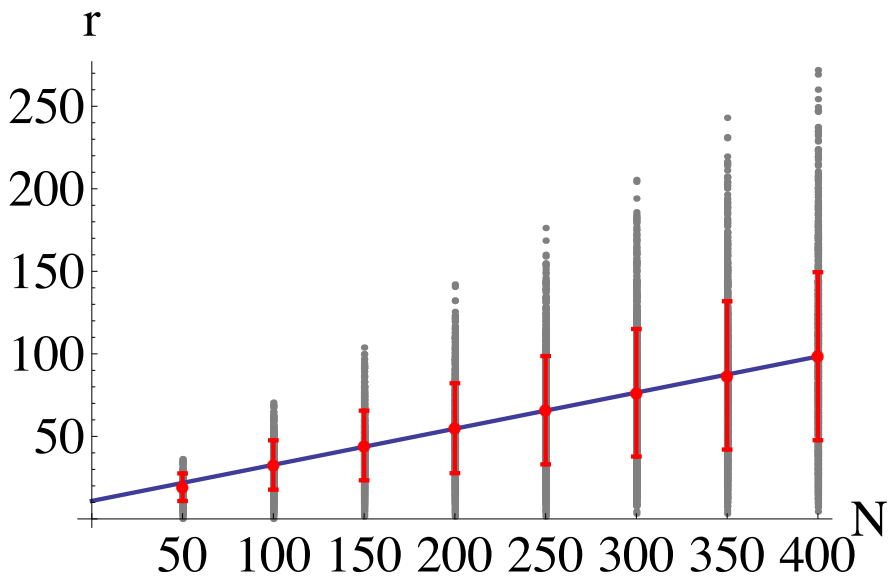

Figure 4.10: Distribution of the radii, r, of 10000 different spreads of OQWs with number of steps, $N = 50$ to $N = 400$. The graph also illustrates the corresponding error bars for specific number of steps as well as the line of best fit determined by the mean values of r for the different N.

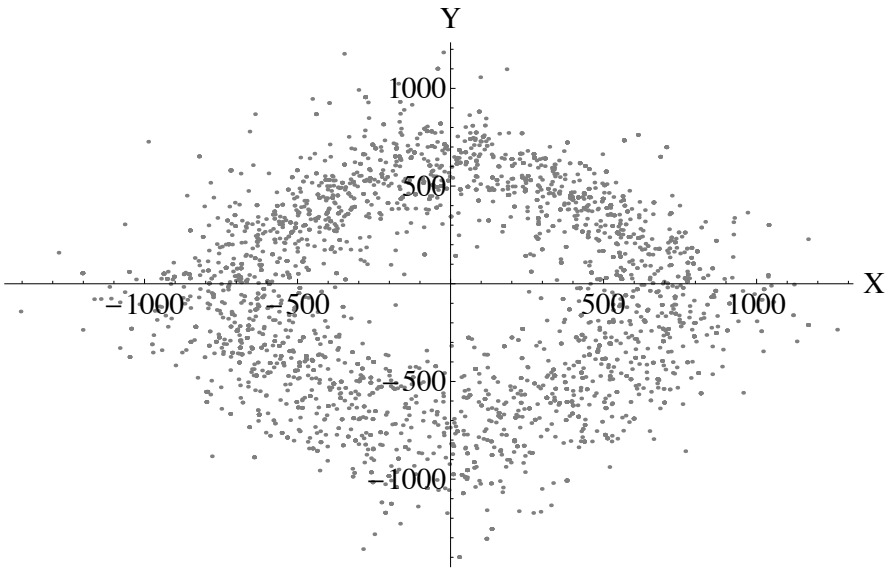

Figure 4.11: Most probable final positions of non-reversal quantum trajectories after 2000 steps. Each end point depends on the quantum coins used to propagate the walk from the origin.

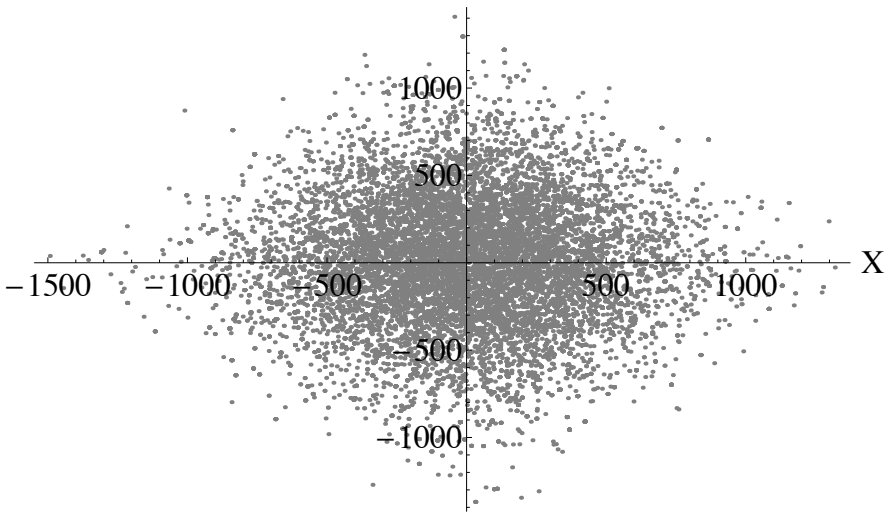

Figure 4.12: Most probable final positions of quantum trajectories (without non-reversal property) after 2000 steps. Each end point depends on the quantum coins used to propagate the walk from the origin.

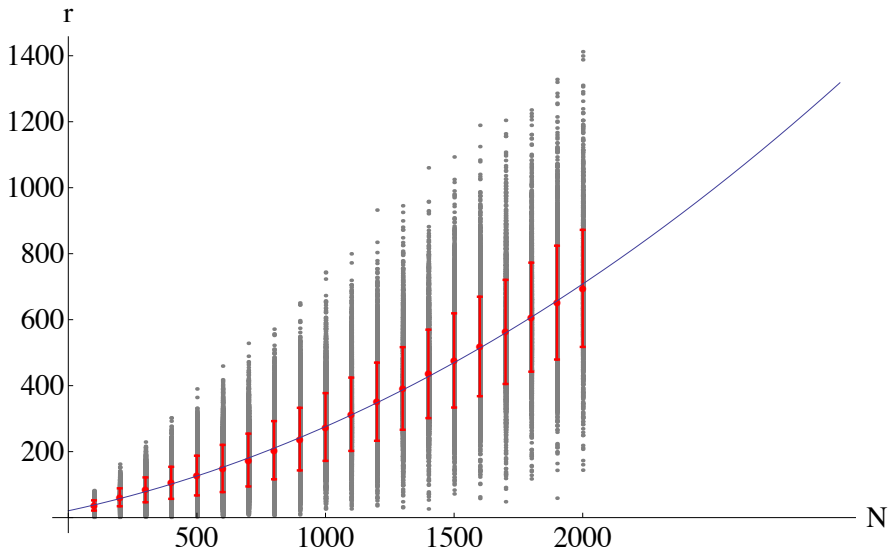

Figure 4.13: Distribution of the radii, r, of 24000 different spreads of non-reversal OQWs each arising from 1000 trajectories with number of steps, $N = 100$ to $N = 2000$. The graph also illustrates the corresponding error bars for specific number of steps as well as an interpolated line of best fit determined by the mean values of r for the different N.

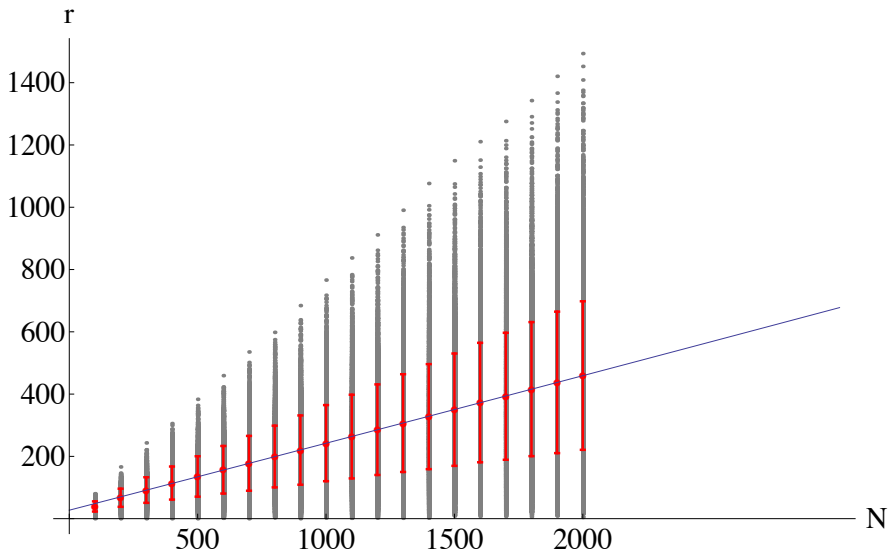

Figure 4.14: Distribution of the radii, r, of 24000 different spreads of OQWs each arising from 1000 trajectories with number of steps, $N = 100$ to $N = 2000$. The graph also illustrates the corresponding error bars for specific number of steps as well as an interpolated line of best fit determined by the mean values of r for the different N.

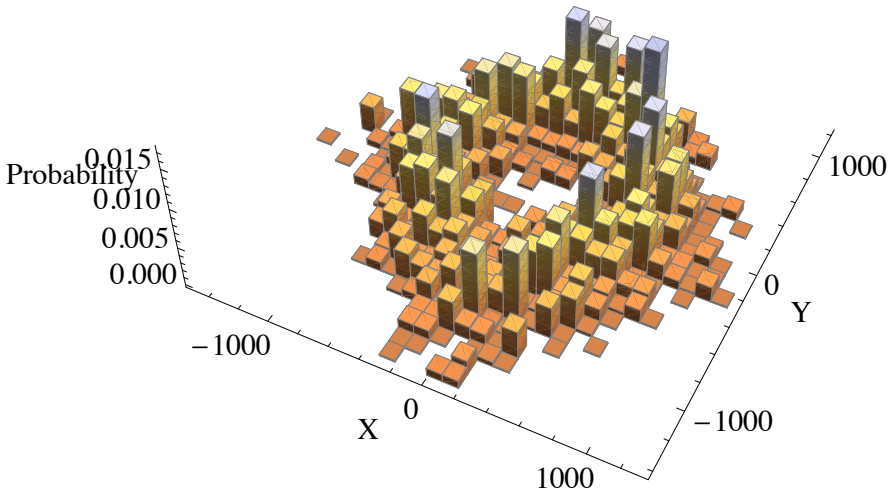

Figure 4.15: Frequency distribution of the end points of non-reversal quantum trajectories after 2000 steps with the origin as starting point. For each trajectory, a different set of quantum coins is used.

Results for larger N

The previous procedures are carried out for $N = 250$ to $N = 2000$. This time, the OQW distributions are produced using quantum trajectories (same principle as for the non-reversal version) to minimise computing power and time. With each of 24000 random unitary matrices, 1000 trajectories undergoing the non-reversal OQW process and another 1000 undergoing the OQW process are generated. Figures 4.11 and 4.12 illustrate their respective ending points on the lattice. The resulting radii distribution are shown in Figures 4.13 and 4.14. The mean values of non-reversal OQW is almost the same as that of ordinary OQW for $N = 100$ to $N = 500$. However, as N grows larger, the mean values tends to have a quadratic increase. The equation of the curves in Figure 4.13 and Figure 4.14 are given in Mathematica by

$$r = 20.7484 + 0.16632N + 8.87039 \times 10^{-5}N^2 \text{ for non-reversal OQW;}$$

$$r = 27.1612 + 0.214204N + 8.90438 \times 10^{-7}N^2 \text{ for OQW.}$$

The frequency distribution diagrams in Figures 4.15 and 4.16 show the spread of the non-reversal OQW and OQW respectively.

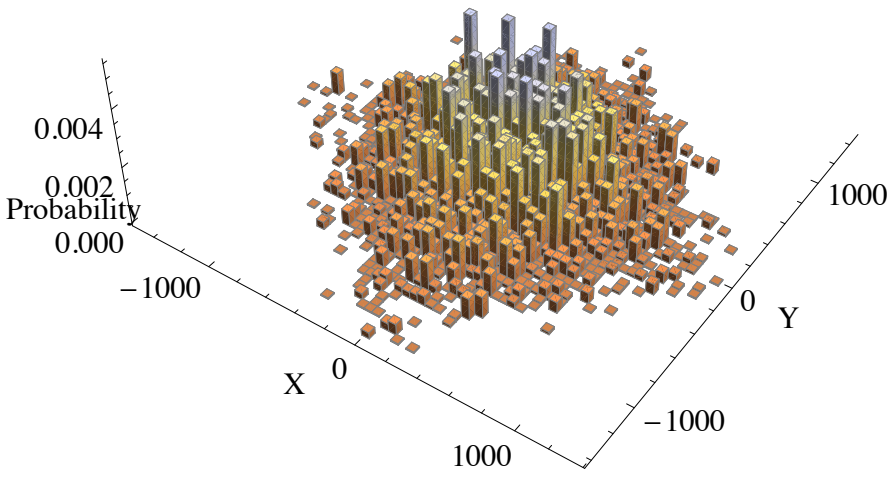

Figure 4.16: Frequency distribution of the end points of quantum trajectories (without non-reversal property) after 2000 steps with the origin as starting point. For each trajectory, a different set of quantum coins is used.

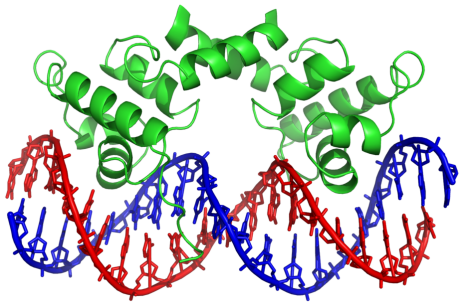

Figure 4.17: DNA: an example of a copolymer (Ref. en.wikipedia.org/wiki/DNA)

4.4 Application in Polymer Physics

In order to demonstrate the relationship between SAWs and polymers, we give a brief review of the relevant part of polymer physics. A more elaborate description of the theory can be found in Flory's manuscripts [50, 51] or in the modern book, Polymer Physics [52].

4.4.1 Polymer chemistry

Poly - mer means many - parts. A polymer is a large chemical structure made up of smaller ones called monomers which are sequentially connected to each other by chemical bonds. Sometimes the monomers may themselves be large units. One such example is the DNA double helix as illustrated in Figure 4.17. Besides DNA, polymers exist in nature in the form of proteins, nucleic acids, sugar and rubber. They are also synthesized in laboratories (e.g. nylon, polystyrene) [53]. Their structures can be classified as homopolymers (composed of identical monomers) or copolymers (composed of different types of monomers). Another way of classifying polymers is as linear or branched. In our work, we only consider linear structures. A typical example is the polyethylene chain.

Polymers with no self-interaction as shown in Figure 4.6 are modeled using the classical random walk. Those with a self-interaction, expressed by the excluded-volume effect, are simulated using the SAW as shown in Figure 4.18. In fact, the excluded-volume effect refers to the property of self-avoidance. In the language of chemistry, it means no position can be occupied by more than one monomer [20]. To sum up, we quote from [53]: "Real chains in good solvents have the same universal features as SAWs on a lattice." In the next section, we investigate about one of the two critical exponents describing these features.

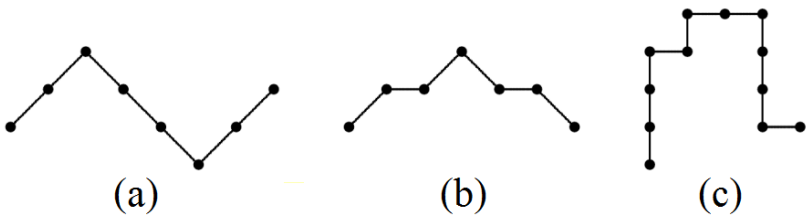

Figure 4.18: Examples of 3 directed paths on $\mathbb{Z}^2$: in combinatorics they are commonly referred to as (a) ballot paths, (b) generalized ballot paths and (c) partially directed SAWs [20].

4.4.2 The critical exponent

Earlier, the radii of the spreads of non-reversal OQWs and OQWs were analysed. When relating random walks to polymers as explained above, the root mean square of the radii gives the end-to-end distance of the polymer, R (not to be confused with the end-to-end distance of the trajectory given by r). Furthermore, the number of steps, N, is equivalent to the size of the polymer. The derivation of the following equations can be found in [54] which is a review of the mathematical perspective of Flory theory for polymers.

$$\langle R^2 \rangle = Nb^2 \text{ (for ideal chain)}, \tag{4.4.1}$$

$$R \sim bN^{\nu} \text{ (for real chain)}, \tag{4.4.2}$$

where b is the Kuhn monomer size (or Kuhn length) as defined in [55, Chapter 25]. It can be interpreted as the distance between two connected sites on the lattice. ν is known as **the critical exponent** that takes values given by the classical Flory formula for dilute linear polymers,

$$\nu = \frac{3}{d+2}, \; d \leq 4, \tag{4.4.3}$$

where d is the dimension of the polymer (or lattice). Formulae for other types of polymers can be found in [56]. Since ν depends only on the dimension in all the formulae, it is referred as a universal exponent. It was named after Flory. For an ideal chain, we have

$$\nu = \begin{cases} 1 & \text{(ballistic motion);} \\ \\ \frac{1}{2} & \text{(diffusive motion).} \end{cases}$$

Thus, the Flory exponent for $d = 2, 3$ lies between the ballistic and diffusive values. For $d = 1$, the SAW exhibits ballistic motion. SAWs in four or higher dimensions behave like classical random walks exhibiting diffusive motion [28]. Before determining the critical exponent of the non-reversal OQW, we define an essential property of the walk.

The fractal dimension

"If a sphere of radius R is drawn with its center in a random position along the chain, the total length of the polymer contained in the sphere is about R^{d_F}" [54]. If d_F is different from the Euclidean dimension, then it is called the fractal dimension [55, Chapter 6]. It is not restricted to being an integer. The fractal dimension provides a statistical measure of the ratio of the space occupied by any fractal object to the space in which it is embedded. More technical definitions and explanation about fractals can be found in the book, The Fractal Geometry of Nature [57]. Usually, a fractal exhibits a certain pattern. As a matter of fact, any SAW is a fractal. Thus, a polymer is a fractal, whereby d_F is then the upper critical dimension above which the excluded volume effect is insignificant.

Determining ν and d_F

In the classical setup, ν is usually determined using graphical method [58]. Firstly, Equation (4.4.2) is transformed into

$$\ln R = \nu \ln N + \ln b. \tag{4.4.4}$$

Secondly, $\ln R$ is plotted against $\ln N$. As a result, the gradient of the graph gives the value of ν and the vertical intercept can be interpreted as $\ln b$. In Mathematica, the equation of the graph can be generated with the help of the function `LinearModelFit`. In the case of the Non-reversal OQW, such an equation is obtained using the data points from Figure 4.19,

$$\ln R = 0.738297 \ln N + 0.233043. \tag{4.4.5}$$

We see that the gradient is approximately equal to the classical Flory exponent for $d = 2$. Using the Normalised Root Mean Square Error (NRMSE), the relative error of the gradient is calculated. Hence, the critical exponent is given by

$$\nu = 0.74 \pm 0.01. \tag{4.4.6}$$

This value determines the mean end-to-end size of a polymer. In classical theory, its reciprocal gives the fractal dimension of the polymer,

$$d_F = 1.35 \pm 0.02. \tag{4.4.7}$$

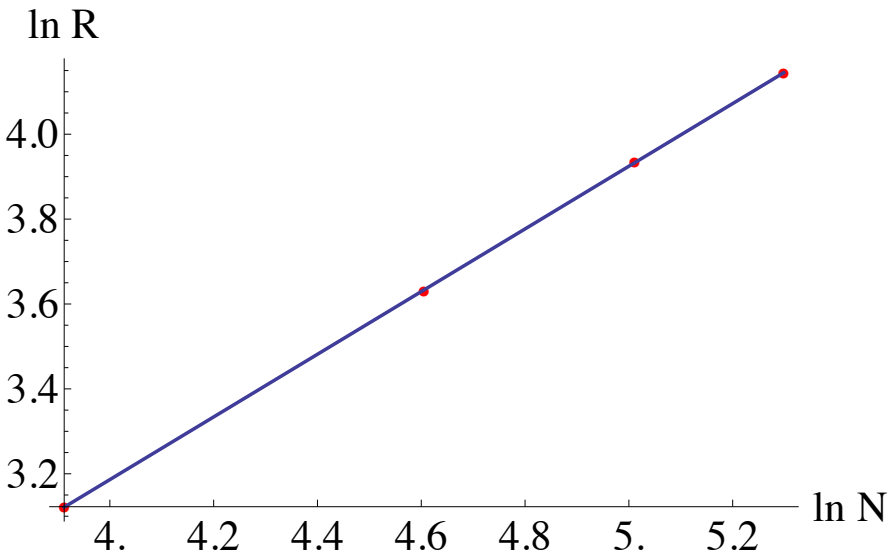

Figure 4.19: Graph of $\ln R$ against $\ln N$ for non-reversal OQW with a maximum of 200 steps. A straight line is fitted to the data points.

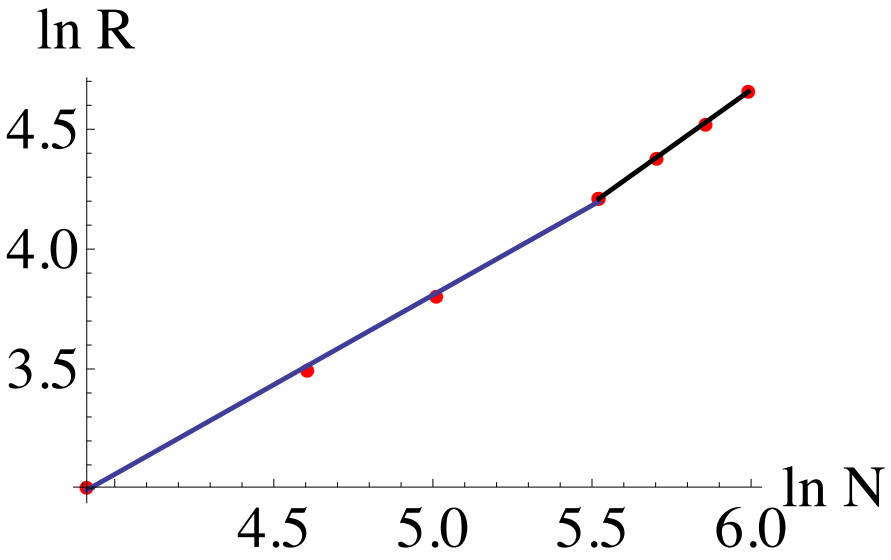

Figure 4.20: Graph of $\ln R$ against $\ln N$ for non-reversal OQW with a maximum of 400 steps. Two straight lines (one in blue and one in black for larger N) are fitted to the data points relevantly. Their gradients differ slightly.

Some approximate classical values of ν obtained in the past are cited in [8] where the author investigates whether ν should always be equal to $\frac{3}{4}$. They range from 0.746 to 0.77 with relative errors ranging from 0.0002 to 0.004. The value determined by the author was

$$\nu = 0.7500 \pm 0.0025. \tag{4.4.8}$$

Other values arising from different Flory-type formulae can be found in the book [59].

In our case, if N is increased to 400, a change in ν occurs as illustrated by the change in gradient in Figure 4.20. In the next section, we investigate further about what happens with larger N to both the OQW and its non-reversal version.

4.4.3 A new formula?

When $\ln R$ is plotted against $\ln N$ for $100 \leq N \leq 2000$, a curve is obtained as shown in Figure 4.21 instead of a straight line. This implies that the the graph for the non-reversal OQW is no more of the typical form of Equation (4.4.4) but rather of a new form,

$$\ln R = A\ln N^2 + B\ln N + C, \tag{4.4.9}$$

where

$$A = 0.140376, \tag{4.4.10}$$

$$B = -0.760841, \tag{4.4.11}$$

$$C = 4.25281. \tag{4.4.12}$$

For the OQW, the values of the coefficients are:

$$A = 0.0367634, \tag{4.4.13}$$

$$B = 0.379127, \tag{4.4.14}$$

$$C = 1.23686. \tag{4.4.15}$$

The corresponding graph is illustrated in Figure 4.22. However, we notice that in both cases, the quadratic curves do not fit the data points perfectly.

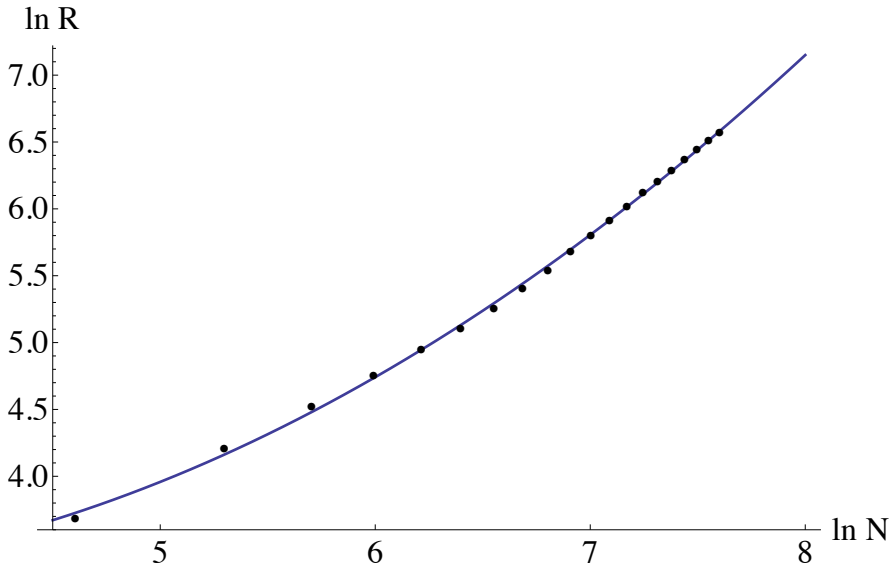

Figure 4.21: Graph of $\ln R$ against $\ln N$ for non-reversal OQW with a maximum of 2000 steps. The blue line is a quadratic curve fitted to the data points.

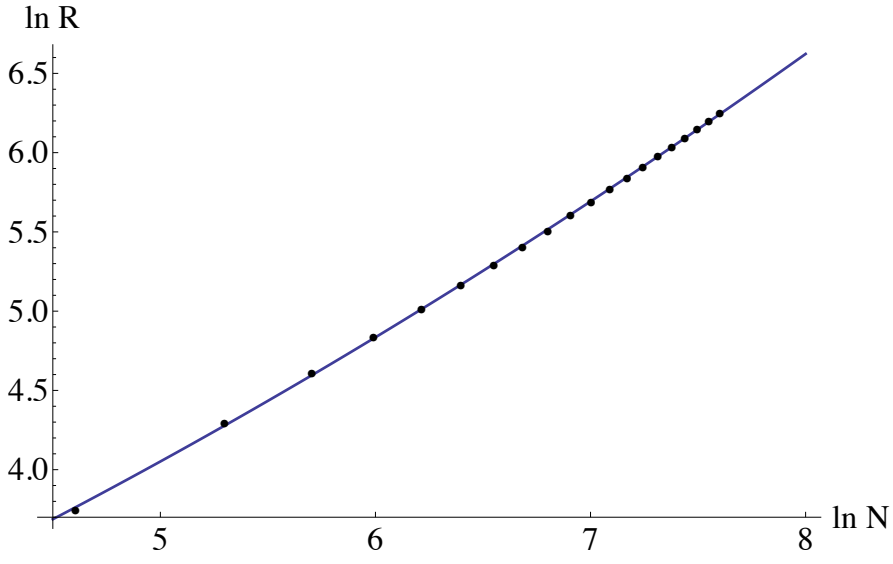

Figure 4.22: Graph of $\ln R$ against $\ln N$ for OQW with a maximum of 2000 steps. The blue line is a quadratic curve fitted to the data points.

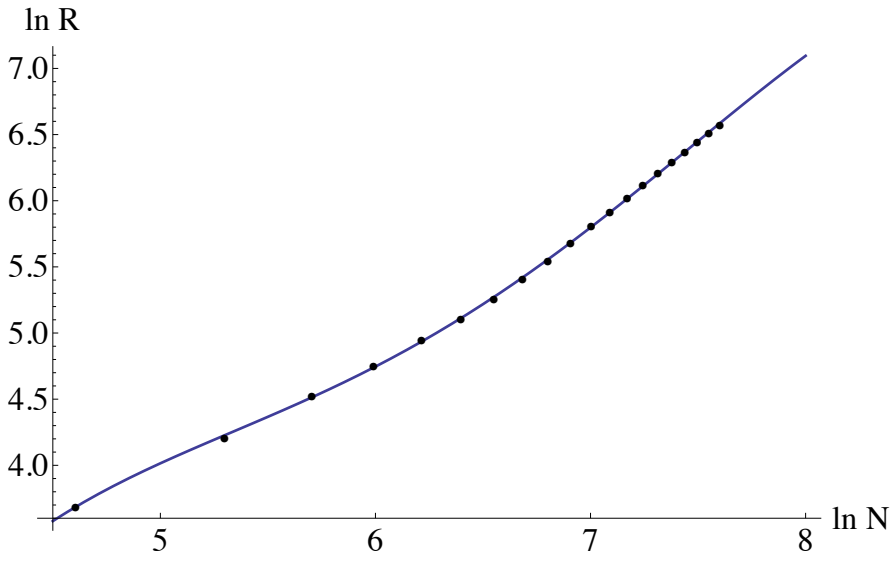

Figure 4.23: Graph of $\ln R$ against $\ln N$ for non-reversal OQW with a maximum of 2000 steps. The blue line is a curve of fourth order fitted to the data points.

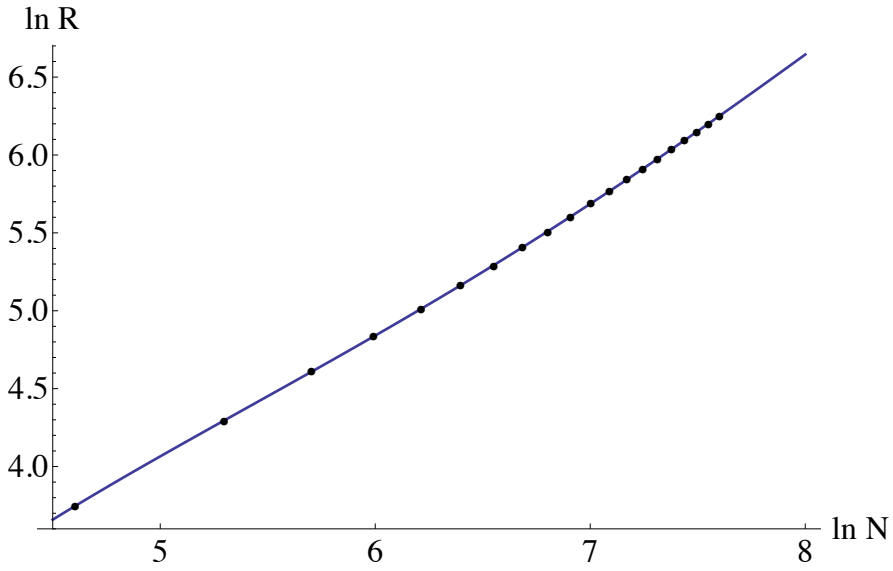

Figure 4.24: Graph of $\ln R$ against $\ln N$ for OQW with a maximum of 2000 steps. The blue line is a curve of fourth order fitted to the data points.

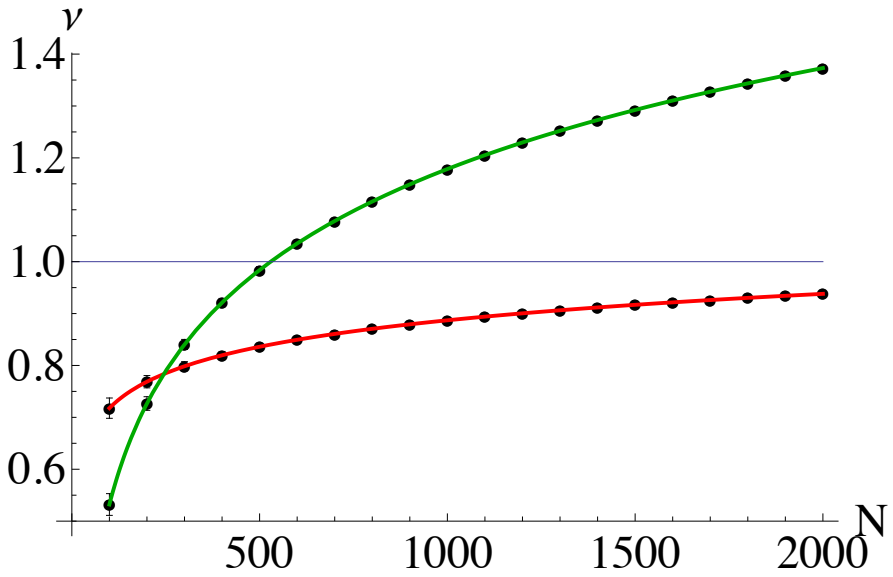

Figure 4.25: The figure shows values of critical exponents for different degree of polymerisation, N, each with their respective error bars. The points on the red line are the values for OQW and those on the green line are for the non-reversal OQW. The line, $\nu = 1$, is a suggested upper bound for OQW that needs to be proven. The two continuous curves arise from logarithmic fits to the respective data sets.

Curves of fourth order as shown in Figures 4.23 and 4.24 are used instead for the non-reversal OQW and OQW respectively. The respective equations are obtained in Mathematica using the function $\texttt{Fit}[DATA, \{1, x, x^2, x^4\}, x]$:

$$\ln R = -47.1805 + 32.5056x - 7.82454x^2 + 0.837709x^3 - 0.0326917x^4,$$

$$\ln R = -8.25094 + 6.22004x - 1.28529x^2 + 0.130484x^3 - 0.00473977x^4,$$

where x is equivalent to $\ln N$. In the future, we shall calculate chi values of the fits of different orders to find out which one is more appropriate. For now, we will assume the best fit to be quadratic to keep the investigation about the exponent simple.

Change in ν

Assuming the derivatives of the curves in Figures 4.21 and 4.22 give values of the critical exponent of the non-reversal OQW and OQW respectively, then the corresponding changes in ν are illustrated in Figure 4.25. From the latter, one can deduce that ν increases faster for the non-reversal OQW. As for the OQW, we would think that ν does not go beyond 1 but this needs to be verified using larger N values. In the classical case, such a limit has been proven for partially directed SAWs [60].

Chapter 5

Conclusion

The non-reversal Open Quantum Walk presented in this thesis is a new model of quantum walk. In the beginning, the project was to develop a Self-Avoiding Walk using the formalism of OQW. At some point, we deduced that it is not easy to have a completely self-avoiding process. The reason has been explained in Chapter 4. Subsequently, we modified our code to make the walk non-reversal. In that case, the process was partially self-avoiding and it respected the property of normalisation condition.

After performing extensive numerics, the statistical results obtained looked very interesting from the point of view of polymer physics. Our aim was to use our model as a substitute of the classical Self-Avoiding Walk used to simulate polymer formation. Our motivation for application was that non-reversal trajectories could go on for very large N unlike the classical SAW. Furthermore, the non-reversal property could be given a physical meaning. It could refer to the "waiting time" in actual polymer formation. Thus, we went ahead to investigate the statistical results of the non-reversal OQW. Alongside, we analysed the corresponding OQWs too.

In the investigation, the typical relationship between degree of polymerisation and end-to-end polymer distance did not stand anymore for large N. Instead of a linear logarithmic relationship, we obtained a quadratic logarithmic relationship. This new hypothesis not only gave rise to multiple sets of questions but needed to be proven.

Prior to making any conclusive statements about new relationship between R and N beyond the classical Flory formula, a more careful study is crucial which is beyond the scope of the present MSc thesis. Therefore, the application of non-reversal OQW in polymer physics requires thorough scrutiny which should include more sophisticated statistical analysis as well as some analytical estimates.

Appendix A

Algorithm and Codes

A.1 Generating "quantum coins"

For an Open Quantum Walk with initial density state of dimension n by n, the "quantum coins" are n by n Kraus operators which can be procured through the procedures below.

Step 1 Generate a random $4n$ by $4n$ unitary matrix, U.

Step 2 From the first (or second or third or fourth) set of n columns of U, construct 4 matrices as follows.
Obtain:

- N using the first n rows,
- S using the second n rows,
- E using the third n rows,
- W using the last n rows.

Step 3 Verify that,

$$N^\dagger N + S^\dagger S + E^\dagger E + W^\dagger W = I.$$

Given that the normalisation condition is fulfilled, then N, S, W, E are the four "quantum coins".

Below is the corresponding Python code used in our research. For simplicity, 2 by 2 complex matrices are generated using the first 2 columns of an 8 by 8 unitary matrix.

```
def randomunitary(n):
   global U;
   M=(np.random.randn(4*n,4*n)
   +1j*np.random.randn(4*n,4*n))/np.sqrt(2);
   q,r=np.linalg.qr(M,mode='complete');
   A=r.diagonal();
   B=[];
   for i in A: B.append(i/abs(i));
   C=np.diag(B);
   U=np.dot(q,C);
   return U;
Unitarymatrix = randomunitary(8);
N=np.matrix([[U[k][l] for l in range (0,2)]
for k in range (0,2)]);
S=np.matrix([[U[k][l] for l in range (0,2)]
for k in range (2,4)]);
E=np.matrix([[U[k][l] for l in range (0,2)]
for k in range (4,6)]);
W=np.matrix([[U[k][l] for l in range (0,2)]
for k in range (6,8)]);
Nh=N.getH();
Sh=S.getH();
Eh=E.getH();
Wh=W.getH();
print(np.around(np.dot(Nh,N)+np.dot(Sh,S)
+np.dot(Eh,E)+np.dot(Wh,W)));
```

A.2 Non-reversal OQW

A.2.1 Mathematica code for 1D

```
Bh=ConjugateTranspose[B];
Fh=ConjugateTranspose[F];

Step[initial_]:={
res=initial;
pB=N[Tr[B.initial[[i]].Bh]];
pF=N[Tr[F.initial[[i]].Bh]];
pcurr=RandomReal[];
If[pcurr<=pB,
If[memo[[i+1]]=={0},
res[[i+1]]=N[B.initial[[i]].Bh/Tr[B.initial[[i]].Bh]];
memo[[i+1]]={1};
i=i+1,
res[[i]]=N[B.initial[[i]].Bh/Tr[B.initial[[i]].Bh]]],
If[memo[[i-1]]=={0},
res[[i-1]]=N[F.initial[[i]].Fh/Tr[F.initial[[i]].Fh]];
memo[[i-1]]={1};
i=i-1,
res[[i]]
=N[F.initial[[i]].Fh/Tr[F.initial[[i]].Fh]]]];
res
}[[1]];

FinalPsi[n_,init_]:={
result=Table[{{0,0},{0,0}},{j,1,2*Msites+1}];
resultT=Table[{{0,0},{0,0}},{j,1,2*Msites+1}];
result=init;
Do[{resultT=Step[result];result=resultT},{k,1,n}];result
}[[1]];
```

```
Msites=101;

probdist[nu_]:={
prob=Table[0,{j,1,2*Msites+1}];
Do[{
psi=Table[{{0,0},{0,0}},{i,1,2*Msites+1}];
memo=Table[{0},{i,1,2*Msites+1}];
psiT=psi;
psi[[Msites+1]]=1/4 {{1,-Sqrt[3]},{-Sqrt[3],3}};
memo[[Msites+1]]={1};
tra=Table[{0},{i,1,2*Msites+1}];
i=Msites+1;
(*Kraus matrices that give single Gaussian and soliton*)
B={{1,0},{0,4/5}};
F={{0,0},{0,3/5}};

(*Kraus matrices that give double Gaussian*)
(*B={{12/13,0},{0,4/5}};
F={{5/13,0},{0,3/5}};*)

S=FinalPsi[Msites-1,psi];prob[[i]]++},{num,1,nu}];
pr=Table[{0,0},{k,1,2*Msites}];
Do[pr[[k]]={k-Msites-1,prob[[k]]/nu},{k,2,2*Msites}];pr
}[[1]];

Datapoints=probdist[50000]
```

A.2.2 Python code for 2D

```
#General functions

#Generating random unitary matrix
def randomunitary(ndim):
    global a
    Mls=(np.random.randn(ndim,ndim)
    +1j*np.random.randn(ndim,ndim))/np.sqrt(2)
    q,r=np.linalg.qr(Mls,mode='complete')
    Sls1=r.diagonal()
    b=[]
    for i in Sls1: b.append(i/abs(i))
    Sls2=np.diag(b)
    a=np.dot(q,Sls2)
    return a;

#trace of a matrix with complex entries
def trace(self):
    t = 0
    for i in range(2):
        t += abs(self[(i,i)])
    return t;

#search for coordinate of endpoint with highest probability
def finalposition(sett):
    global Msites
    (x1,y1)=np.unravel_index(sett.argmax(), sett.shape)
    return (y1-Msites-1,x1-Msites-1)
```

```
#OQW FUNCTIONS

#step function for OQW trajectory
def oqwFun(result):
    global R, i, j, F, W, M, S, Fh, Wh, Mh, Sh, oLT

    rF=np.dot(F, np.dot(result[j][i],Fh));
    rW=np.dot(W, np.dot(result[j][i],Wh));
    rM=np.dot(M, np.dot(result[j][i],Mh));
    rS=np.dot(S, np.dot(result[j][i],Sh));

    pF=trace(rF);
    pW=trace(rW);
    pM=trace(rM);
    pS=trace(rS);

    if pF != 0: Rig = rF/pF;
    else: print(0)
    if pW != 0: Lef = rW/pW;
    else: print(0)
    if pM != 0: Upp = rM/pM;
    else: print(0)
    if pS != 0: Dow = rS/pS;
    else: print(0)

    pcurr=np.random.random_sample();
    if 0 < pcurr <= pF:
        result[j][i+1] = Rig; oLT.append([i+1,j]); i=i+1;

    elif pF < pcurr <= pF + pW:
        result[j][i-1] = Lef; oLT.append([i-1,j]); i=i-1;

    elif pF + pW < pcurr <= pF + pW + pM:
        result[j+1][i] = Upp; oLT.append([i,j+1]); j=j+1;
    else:
        result[j-1][i] = Dow; oLT.append([i,j-1]); j=j-1;
    return result;
```

```
#Generating OQW trajectories
def oqwFin(n,ini):
   global ff1, ff2, ff3, ff4, ff5, ff6, ff7, ff8, ff9, ff10,
   ff11, ff12, ff13, ff14, ff15, ff16, ff17, ff18, ff19, Msites
   global opro1, opro2, opro3, opro4, opro5,
   opro6, opro7, opro8, opro9, opro10,
   opro11, opro12, opro13, opro14, opro15,
   opro16, opro17, opro18, opro19
   global oLT, i, j

   resT=np.empty((2*Msites + 1,2*Msites + 1,2,2))+0j;
   res=ini;
   for k in range (0,n):
       resT = oqwFun(res);
       res = resT;
       if len(oLT) == ff1 : opro1[j][i]+=1;
       if len(oLT) == ff2 : opro2[j][i]+=1;
       if len(oLT) == ff3 : opro3[j][i]+=1;
       if len(oLT) == ff4 : opro4[j][i]+=1;
       if len(oLT) == ff5 : opro5[j][i]+=1;
       if len(oLT) == ff6 : opro6[j][i]+=1;
       if len(oLT) == ff7 : opro7[j][i]+=1;
       if len(oLT) == ff8 : opro8[j][i]+=1;
       if len(oLT) == ff9 : opro9[j][i]+=1;
       if len(oLT) == ff10 : opro10[j][i]+=1;
       if len(oLT) == ff11 : opro11[j][i]+=1;
       if len(oLT) == ff12 : opro12[j][i]+=1;
       if len(oLT) == ff13 : opro13[j][i]+=1;
       if len(oLT) == ff14 : opro14[j][i]+=1;
       if len(oLT) == ff15 : opro15[j][i]+=1;
       if len(oLT) == ff16 : opro16[j][i]+=1;
       if len(oLT) == ff17 : opro17[j][i]+=1;
       if len(oLT) == ff18 : opro18[j][i]+=1;
       if len(oLT) == ff19 : opro19[j][i]+=1;

   return res;
```

```
#generating many realisations of OQW trajectories
#and recording final positions after specific number of steps
def oqwprobdist(nu):
    global ff1, ff2, ff3, ff4, ff5, ff6, ff7, ff8, ff9, ff10,
    ff11, ff12, ff13, ff14, ff15, ff16, ff17, ff18, ff19, Msites
    global opro1, opro2, opro3, opro4, opro5,
    opro6, opro7, opro8, opro9, opro10,opro11, opro12, opro13,
    opro14, opro15, opro16, opro17, opro18, opro19
    global psi, j, i, oLT, UnionradiusoN,UnionradiusoP

    opro1 = np.zeros((2*Msites + 1,2*Msites + 1));
    opro2 = np.zeros((2*Msites + 1,2*Msites + 1));
    opro3 = np.zeros((2*Msites + 1,2*Msites + 1));
    opro4 = np.zeros((2*Msites + 1,2*Msites + 1));
    opro5 = np.zeros((2*Msites + 1,2*Msites + 1));
    opro6 = np.zeros((2*Msites + 1,2*Msites + 1));
    opro7 = np.zeros((2*Msites + 1,2*Msites + 1));
    opro8 = np.zeros((2*Msites + 1,2*Msites + 1));
    opro9 = np.zeros((2*Msites + 1,2*Msites + 1));
    opro10 = np.zeros((2*Msites + 1,2*Msites + 1));
    opro11 = np.zeros((2*Msites + 1,2*Msites + 1));
    opro12 = np.zeros((2*Msites + 1,2*Msites + 1));
    opro13 = np.zeros((2*Msites + 1,2*Msites + 1));
    opro14 = np.zeros((2*Msites + 1,2*Msites + 1));
    opro15 = np.zeros((2*Msites + 1,2*Msites + 1));
    opro16 = np.zeros((2*Msites + 1,2*Msites + 1));
    opro17 = np.zeros((2*Msites + 1,2*Msites + 1));
    opro18 = np.zeros((2*Msites + 1,2*Msites + 1));
    opro19 = np.zeros((2*Msites + 1,2*Msites + 1));
    opro  = np.zeros((2*Msites + 1,2*Msites + 1));

    for k in range (0,nu):
        psi=np.empty((2*Msites + 1,2*Msites + 1,2,2))+0j;
        i=j=Msites + 1;
        psi[j][i]=(1/4)*np.matrix([[1, -np.sqrt(3)],[-np.sqrt(3), 3]]);
        oLT=[[i,j]];
        oqwFin(Msites-1,psi);
        if len(oLT) == Msites:
            opro[j][i]+=1;
```

```
        break;

dispOQW1 = finalposition(opro1);dispOQW2 = finalposition(opro2);
dispOQW3 = finalposition(opro3);dispOQW4 = finalposition(opro4);
dispOQW5 = finalposition(opro5);dispOQW6 = finalposition(opro6);
dispOQW7 = finalposition(opro7);dispOQW8 = finalposition(opro8);
dispOQW9 = finalposition(opro9);dispOQW10 = finalposition(opro10);
dispOQW11 = finalposition(opro11);dispOQW12 = finalposition(opro12);
dispOQW13 = finalposition(opro13);dispOQW14 = finalposition(opro14);
dispOQW15 = finalposition(opro15);dispOQW16 = finalposition(opro16);
dispOQW17 = finalposition(opro17);dispOQW18 = finalposition(opro18);
dispOQW19 = finalposition(opro19);dispOQW = finalposition(opro);

norm1 = LA.norm(dispOQW1);norm2 = LA.norm(dispOQW2);
norm3 = LA.norm(dispOQW3);norm4 = LA.norm(dispOQW4);
norm5 = LA.norm(dispOQW5);norm6 = LA.norm(dispOQW6);
norm7 = LA.norm(dispOQW7);norm8 = LA.norm(dispOQW8);
norm9 = LA.norm(dispOQW9);norm10 = LA.norm(dispOQW10);
norm11 = LA.norm(dispOQW11);norm12 = LA.norm(dispOQW12);
norm13 = LA.norm(dispOQW13);norm14 = LA.norm(dispOQW14);
norm15 = LA.norm(dispOQW15);norm16 = LA.norm(dispOQW16);
norm17 = LA.norm(dispOQW17);norm18 = LA.norm(dispOQW18);
norm19 = LA.norm(dispOQW19);normf = LA.norm(dispOQW);

f1f2f3norm = [(ff1 - 1, norm1),(ff2 - 1, norm2),(ff3 - 1, norm3),
              (ff4 - 1, norm4),(ff5 - 1, norm5),(ff6 - 1, norm6),
              (ff7 - 1, norm7),(ff8 - 1, norm8),(ff9 - 1, norm9),
              (ff10 - 1, norm10),(ff11 - 1, norm11),
              (ff12 - 1, norm12),(ff13 - 1, norm13),
              (ff14 - 1, norm14),(ff15 - 1, norm15),
              (ff16 - 1, norm16),(ff17 - 1, norm17),
              (ff18 - 1, norm18),(ff19 - 1, norm19),
              (Msites - 1, normf)];

UnionradiusoN = set(UnionradiusoN) | set(f1f2f3norm);
UnionradiusoP = set(UnionradiusoP) | {dispOQW};
return ;
```

```
#NOQW FUNCTIONS

#Checking for free sites around
def Test(tra):
    global R, i, j
    R=[];
    if tra[j][i+1] == 0: R.append("ri");
    if tra[j][i-1] == 0: R.append("le");
    if tra[j-1][i] == 0: R.append("d");
    if tra[j+1][i] == 0: R.append("u");
    return R;

#Step function for NOQW trajectory
def Fun(result):
    global R, i, j, F, W, M, S, Fh, Wh, Mh, Sh, memo, LT

    rF=np.dot(F, np.dot(result[j][i],Fh));
    rW=np.dot(W, np.dot(result[j][i],Wh));
    rM=np.dot(M, np.dot(result[j][i],Mh));
    rS=np.dot(S, np.dot(result[j][i],Sh));

    pF=trace(rF);pW=trace(rW);pM=trace(rM);pS=trace(rS);

    if pF != 0: Rig = rF/pF;
    else: print(0)
    if pW != 0: Lef = rW/pW;
    else: print(0)
    if pM != 0: Upp = rM/pM;
    else: print(0)
    if pS != 0: Dow = rS/pS;
    else: print(0)

    pcurr=np.random.random_sample();
    if 0 < pcurr <= pF:
        if "ri" in R:
            result[j][i+1] = Rig;
            memo[j][i+1] = 1;
            LT.append([i+1,j]);
```

```
        i=i+1;
    else: result[j][i] = Rig; LT.append([i,j]);

elif pF < pcurr <= pF + pW:
    if "le" in R:
        result[j][i-1] = Lef;
        memo[j][i-1] = 1; LT.append([i-1,j]); i=i-1;
    else: result[j][i] = Lef; LT.append([i,j]);

elif pF + pW < pcurr <= pF + pW + pM:
    if "u" in R:
        result[j+1][i] = Upp;
        memo[j+1][i] = 1; LT.append([i,j+1]); j=j+1;
    else: result[j][i] = Upp; LT.append([i,j]);

else:
    if "d" in R:
        result[j-1][i] = Dow;
        memo[j-1][i] = 1; LT.append([i,j-1]); j=j-1;
    else: result[j][i] = Dow; LT.append([i,j]);

return result;
```

```
#Generating NOQW trajectory
def Fin(n,ini):
    global ff1, ff2, ff3, ff4, ff5, ff6, ff7, ff8, ff9, ff10,
    ff11, ff12, ff13, ff14, ff15, ff16, ff17, ff18, ff19, Msites
    global prob1, prob2, prob3, prob4, prob5,
    prob6, prob7, prob8, prob9, prob10,prob11, prob12, prob13,
    prob14, prob15, prob16, prob17, prob18, prob19
    global memo, LT, i, j

    memo=np.zeros((2*Msites + 1,2*Msites + 1));
    memo[j][i]=1;
    resT=np.empty((2*Msites + 1,2*Msites + 1,2,2))+0j;
    res=ini;
    for k in range (0,n):
        R=Test(memo);
        if R!=[]:
            resT = Fun(res);
            res = resT;
            if len(LT) == ff1 : prob1[j][i]+=1;
            if len(LT) == ff2 : prob2[j][i]+=1;
            if len(LT) == ff3 : prob3[j][i]+=1;
            if len(LT) == ff4 : prob4[j][i]+=1;
            if len(LT) == ff5 : prob5[j][i]+=1;
            if len(LT) == ff6 : prob6[j][i]+=1;
            if len(LT) == ff7 : prob7[j][i]+=1;
            if len(LT) == ff8 : prob8[j][i]+=1;
            if len(LT) == ff9 : prob9[j][i]+=1;
            if len(LT) == ff10 : prob10[j][i]+=1;
            if len(LT) == ff11 : prob11[j][i]+=1;
            if len(LT) == ff12 : prob12[j][i]+=1;
            if len(LT) == ff13 : prob13[j][i]+=1;
            if len(LT) == ff14 : prob14[j][i]+=1;
            if len(LT) == ff15 : prob15[j][i]+=1;
            if len(LT) == ff16 : prob16[j][i]+=1;
            if len(LT) == ff17 : prob17[j][i]+=1;
            if len(LT) == ff18 : prob18[j][i]+=1;
            if len(LT) == ff19 : prob19[j][i]+=1;
        else: break;
    return res;
```

```
#Generating many realisations of NOQW trajectories
#and recording endpoints after specific number of steps
def probdist(nu):
    global ff1, ff2, ff3, ff4, ff5, ff6, ff7, ff8, ff9, ff10,
    ff11, ff12, ff13, ff14, ff15, ff16, ff17, ff18, ff19, Msites
    global prob1, prob2, prob3, prob4, prob5,
    prob6, prob7, prob8, prob9, prob10,
    prob11, prob12, prob13, prob14, prob15,
    prob16, prob17, prob18, prob19
    global nur, psi, j, i, LT, UnionradiusN,UnionradiusP

    nur=9;

    prob1 = np.zeros((2*Msites + 1,2*Msites + 1));
    prob2 = np.zeros((2*Msites + 1,2*Msites + 1));
    prob3 = np.zeros((2*Msites + 1,2*Msites + 1));
    prob4 = np.zeros((2*Msites + 1,2*Msites + 1));
    prob5 = np.zeros((2*Msites + 1,2*Msites + 1));
    prob6 = np.zeros((2*Msites + 1,2*Msites + 1));
    prob7 = np.zeros((2*Msites + 1,2*Msites + 1));
    prob8 = np.zeros((2*Msites + 1,2*Msites + 1));
    prob9 = np.zeros((2*Msites + 1,2*Msites + 1));
    prob10 = np.zeros((2*Msites + 1,2*Msites + 1));
    prob11 = np.zeros((2*Msites + 1,2*Msites + 1));
    prob12 = np.zeros((2*Msites + 1,2*Msites + 1));
    prob13 = np.zeros((2*Msites + 1,2*Msites + 1));
    prob14 = np.zeros((2*Msites + 1,2*Msites + 1));
    prob15 = np.zeros((2*Msites + 1,2*Msites + 1));
    prob16 = np.zeros((2*Msites + 1,2*Msites + 1));
    prob17 = np.zeros((2*Msites + 1,2*Msites + 1));
    prob18 = np.zeros((2*Msites + 1,2*Msites + 1));
    prob19 = np.zeros((2*Msites + 1,2*Msites + 1));
    prob  = np.zeros((2*Msites + 1,2*Msites + 1));

    for k in range (0,nu):
        psi=np.empty((2*Msites + 1,2*Msites + 1,2,2))+0j;
        i=j=Msites + 1;
        psi[j][i]=(1/4)*np.matrix([[1, -np.sqrt(3)],[-np.sqrt(3), 3]]);
```

```
        LT=[[i,j]];
        Fin(Msites-1,psi);
        if len(LT) == Msites:
            prob[j][i]+=1;

    if LT!=[[-Msites-1,-Msites-1]]:
        nur=1;
        dispNOQW1 = finalposition(prob1);
        dispNOQW2 = finalposition(prob2);
        dispNOQW3 = finalposition(prob3);
        dispNOQW4 = finalposition(prob4);
        dispNOQW5 = finalposition(prob5);
        dispNOQW6 = finalposition(prob6);
        dispNOQW7 = finalposition(prob7);
        dispNOQW8 = finalposition(prob8);
        dispNOQW9 = finalposition(prob9);
        dispNOQW10 = finalposition(prob10);
        dispNOQW11 = finalposition(prob11);
        dispNOQW12 = finalposition(prob12);
        dispNOQW13 = finalposition(prob13);
        dispNOQW14 = finalposition(prob14);
        dispNOQW15 = finalposition(prob15);
        dispNOQW16 = finalposition(prob16);
        dispNOQW17 = finalposition(prob17);
        dispNOQW18 = finalposition(prob18);
        dispNOQW19 = finalposition(prob19);
        dispNOQW = finalposition(prob);

        norm1 = LA.norm(dispNOQW1);norm2 = LA.norm(dispNOQW2);
        norm3 = LA.norm(dispNOQW3);norm4 = LA.norm(dispNOQW4);
        norm5 = LA.norm(dispNOQW5);norm6 = LA.norm(dispNOQW6);
        norm7 = LA.norm(dispNOQW7);norm8 = LA.norm(dispNOQW8);
        norm9 = LA.norm(dispNOQW9);norm10 = LA.norm(dispNOQW10);
        norm11 = LA.norm(dispNOQW11);norm12 = LA.norm(dispNOQW12);
        norm13 = LA.norm(dispNOQW13);norm14 = LA.norm(dispNOQW14);
        norm15 = LA.norm(dispNOQW15);norm16 = LA.norm(dispNOQW16);
        norm17 = LA.norm(dispNOQW17);norm18 = LA.norm(dispNOQW18);
        norm19 = LA.norm(dispNOQW19);normf = LA.norm(dispNOQW);
```

```
f1f2f3norm = [(ff1 - 1, norm1),(ff2 - 1, norm2),(ff3 - 1, norm3),
              (ff4 - 1, norm4),(ff5 - 1, norm5),(ff6 - 1, norm6),
              (ff7 - 1, norm7),(ff8 - 1, norm8),(ff9 - 1, norm9),
              (ff10 - 1, norm10),(ff11 - 1, norm11),
              (ff12 - 1, norm12),(ff13 - 1, norm13),
              (ff14 - 1, norm14),(ff15 - 1, norm15),
              (ff16 - 1, norm16),(ff17 - 1, norm17),
              (ff18 - 1, norm18),(ff19 - 1, norm19),
              (Msites - 1, normf)];


UnionradiusN = set(UnionradiusN) | set(f1f2f3norm);
UnionradiusP = set(UnionradiusP) | {dispNOQW};

return ;
```

```
# MAIN FUNCTION

def fds(xxx):
    xcx,id=xxx
    np.random.seed(int(time()+id))
    #random seed is very important in parallel processing
    #to prevent duplication of results on same node

    global F, W, M, S, Fh, Wh, Mh, Sh, Msites
    global UnionradiusoN,UnionradiusoP, UnionradiusN,UnionradiusP

    UnionradiusoN={};  #record radii for OQW
    UnionradiusoP={};  #record final point for OQW
    UnionradiusN={};   #record radii for NOQW
    UnionradiusP={};   #record final point for NOQW

#launching OQWs and NOQWs starting with different unitary matrices

    for k in range (xcx):
        U = randomunitary(8);
        M=np.matrix([[U[k][l] for l in range (0,2)]for k in range (0,2)])
        S=np.matrix([[U[k][l] for l in range (0,2)]for k in range (2,4)])
        F=np.matrix([[U[k][l] for l in range (0,2)]for k in range (4,6)])
        W=np.matrix([[U[k][l] for l in range (0,2)]for k in range (6,8)])
        Mh=M.getH()
        Sh=S.getH()
        Fh=F.getH()
        Wh=W.getH()

        LisNoqw = probdist(nu);    #launching NOQW realisations first
        Lisoqw =  oqwprobdist(nu);  #followed by OQW realisations

    #at this point the output are being appended into a text file.
    f = open('oqwnoqw.txt', 'a')
    f.write(' \n')
    f.write(str([[UnionradiusoN,UnionradiusoP],[UnionradiusN,UnionradiusP]]))
    f.write(' \n')
    f.close()
    return;
```

```
#the following are the inputs:
#modules needed
import numpy as np
from numpy import linalg as LA
#import matplotlib
#from matplotlib import pylab
import multiprocessing
from multiprocessing import Pool
from time import time

#for testing
#Msites,ff1,ff2,ff3,ff4,ff5,ff6,ff7,ff8,ff9,ff10,
ff11,ff12,ff13,ff14,ff15,ff16,ff17,ff18,ff19,nu
=25,4,5,6,7,8,9,10,11,12,13,14,15,16,17,18,19,20,21,22,10

'''if __name__ == '__main__':
    with Pool() as p:
        p.map(fds, [(2,0),(2,1),(2,2),(2,3),(2,4),(2,5),
        (2,6),(2,7),(2,8),(2,9),(2,10),
        (2,11),(2,12),(2,13),(2,14),(2,15),
        (2,16),(2,17),(2,18),(2,19)])'''

#for cluster
Msites,ff1,ff2,ff3,ff4,ff5,ff6,ff7,ff8,ff9,ff10,
ff11,ff12,ff13,ff14,ff15,ff16,ff17,ff18,ff19,nu
=2001,101,201,301,401,501,601,701,801,901,1001,
1101,1201,1301,1401,1501,1601,1701,1801,1901,1000
#4001,201,401,601,801,1001,1201,1401,1601,1801,2001,
2201,2401,2601,2801,3001,3201,3401,3601,3801,1000

#launched on 1 node having 20 cores

if __name__ == '__main__':
    with Pool() as p:
        p.map(fds, [(15,0),(15,1),(15,2),(15,3),(15,4),(15,5),
        (15,6),(15,7),(15,8),(15,9),(15,10),
        (15,11),(15,12),(15,13),(15,14),(15,15),
        (15,16),(15,17),(15,18),(15,19)])
```

References

[1] Hayes, B., 1998. How to avoid yourself. American Scientist, 86(4), p.314.

[2] Bachelier, L., 2011. Louis Bachelier's theory of speculation: the origins of modern finance. Princeton University Press.

[3] Einstein, A., 1956. Investigations on the Theory of the Brownian Movement. Dover Publications.

[4] Von Smoluchowski, M., 1906. Zur kinetischen theorie der Brownschen molekularbewegung und der suspensionen. Annalen der physik, 326(14), pp.756-780.

[5] Orr, W.J.C., 1947. Statistical treatment of polymer solutions at infinite dilution. Transactions of the Faraday Society, 43, pp.12-27.

[6] Flory, P.J., 1949. The configuration of real polymer chains. The Journal of Chemical Physics, 17(3), pp.303-310.

[7] Webb, B.Z. and Cohen, E.G.D., 2014. Self-avoiding modes of motion in a deterministic Lorentz lattice gas. Journal of Physics A: Mathematical and Theoretical, 47(31), p.315202.

[8] Djordjevic, Z.V., Majid, I., Stanley, H.E. and Dos Santos, R.J., 1983. Correction-to-scaling exponents and amplitudes for the correlation length of linear polymers in two dimensions. Journal of Physics A: Mathematical and General, 16(14), p.L519.

[9] Hueter, I., 2001. Proof of the conjecture that the planar self-avoiding walk has root mean square displacement exponent 3/4. arXiv preprint math/0108077.

[10] Glazman, A., 2015. Connective constant for a weighted self-avoiding walk on $\mathbb{Z}^2$. Electronic Communications in Probability, 20, pp.1-13.

[11] Beaton, N.R., Guttmann, A.J. and Jensen, I., 2012. A numerical adaptation of self-avoiding walk identities from the honeycomb to other 2D lattices. Journal of Physics A Mathematical General, 45(3), p.5201.

[12] Machida, T., Chandrashekar, C.M., Konno, N. and Busch, T., 2013. Self-avoiding quantum walks: realisations in subspaces and limit theorems. arXiv preprint arXiv:1307.6288.

[13] Proctor, T.J., Barr, K.E., Hanson, B., Martiel, S., Pavlovic, V., Bullivant, A. and Kendon, V.M., 2014. Nonreversal and nonrepeating quantum walks. Physical Review A, 89(4), p.042332.

[14] Camilleri, E., Rohde, P.P. and Twamley, J., 2014. Quantum walks with tuneable self-avoidance in one dimension. Scientific reports, 4.

[15] Breuer, H.P. and Petruccione, F., 2002. The theory of open quantum systems. Oxford University Press.

[16] Attal, S., Petruccione, F., Sabot, C. and Sinayskiy, I., 2012. Open quantum random walks. Journal of Statistical Physics, 147(4), pp.832-852.

[17] Venegas-Andraca, S., 2008. Quantum Walks for Computer Scientists. Morgan and Claypool Publishers.

[18] Nielsen, M.A. and Chuang, I.L., 2010. Quantum computation and quantum information. Cambridge university press.

[19] Grover, L.K., 1997. Quantum mechanics helps in searching for a needle in a haystack. Physical review letters, 79(2), p.325.

[20] Den Hollander, F., 2009. Random Polymers: cole dt de Probabilits de Saint-Flour XXXVII2007. Springer-Verlag.

[21] Kendon, V.M., 2006. A random walk approach to quantum algorithms. Philosophical Transactions of the Royal Society of London A: Mathematical, Physical and Engineering Sciences, 364(1849), pp.3407-3422.

[22] Shor, P.W., 1999. Polynomial-time algorithms for prime factorization and discrete logarithms on a quantum computer. SIAM review, 41(2), pp.303-332.

[23] Bauer, H., 1996. Probability Theory, Vol. 23 of De Gruyter Studies in Mathematics. Walter de Gruyter Co.

[24] Guttmann, A.J., 2012. Self-avoiding walks and polygons - an overview. Asia Pacific Mathematics Newsletter, 2, World Scientific Publishing Co.

[25] Van der Hofstad, R. and Slade, G., 2003. Convergence of critical oriented percolation to super-Brownian motion above 4+1 dimensions. In Annales de l'IHP Probabilits et statistiques (Vol. 39, No. 3, pp. 413-485).

[26] Madras, N. and Slade, G., 2013. The self-avoiding walk. Springer Science & Business Media.

[27] Chen, M. and Lin, K.Y., 2002. Universal amplitude ratios for three-dimensional self-avoiding walks. Journal of Physics A: Mathematical and General, 35(7), p.1501.

[28] Hara, T. and Slade, G., 1992. Self-avoiding walk in five or more dimensions I. The critical behaviour. Communications in Mathematical Physics, 147(1), pp.101-136.

[29] Aharonov, Y., Davidovich, L. and Zagury, N., 1993. Quantum random walks. Physical Review A, 48(2), p.1687.

[30] Kempe, J., 2009. Quantum random walks: an introductory overview. Contemporary Physics, 50(1), pp.339-359.

[31] Bergou, J.A. and Hillery, M., 2013. Introduction to the theory of quantum information processing. Springer Science & Business Media.

[32] Ambainis, A., 2003. Quantum walks and their algorithmic applications. International Journal of Quantum Information, 1(04), pp.507-518.

[33] Poulios, K., Keil, R., Fry, D., Meinecke, J.D., Matthews, J.C., Politi, A., Lobino, M., Gräfe, M., Heinrich, M., Nolte, S. and Szameit, A., 2014. Quantum walks of correlated photon pairs in two-dimensional waveguide arrays. Physical review letters, 112(14), p.143604.

[34] Dür, W., Raussendorf, R., Kendon, V.M. and Briegel, H.J., 2002. Quantum walks in optical lattices. Physical Review A, 66(5), p.052319.

[35] Hildner, R., Brinks, D., Nieder, J.B., Cogdell, R.J. and van Hulst, N.F., 2013. Quantum coherent energy transfer over varying pathways in single light-harvesting complexes. Science, 340(6139), pp.1448-1451.

[36] Engel, G.S., Calhoun, T.R., Read, E.L., Ahn, T.K., Mancal, T., Cheng, Y.C., Blankenship, R.E. and Fleming, G.R., 2007. Evidence for wavelike energy transfer through quantum coherence in photosynthetic systems. Nature, 446(7137), pp.782-786.

[37] Aharonov, D., Ambainis, A., Kempe, J. and Vazirani, U., 2001, July. Quantum walks on graphs. In Proceedings of the thirty-third annual ACM symposium on Theory of computing (pp. 50-59). ACM.

[38] Kempe, J., 2005. Discrete quantum walks hit exponentially faster. Probability theory and related fields, 133(2), pp.215-235.

[39] Childs, A.M., Farhi, E. and Gutmann, S., 2002. An example of the difference between quantum and classical random walks. Quantum Information Processing, 1(1-2), pp.35-43.

[40] Wang, J. and Manouchehri, K., 2013. Physical implementation of quantum walks. Springer.

[41] Mülken, O. and Blumen, A., 2011. Continuous-time quantum walks: Models for coherent transport on complex networks. Physics Reports, 502(2), pp.37-87.

[42] Attal, S., Petruccione, F. and Sinayskiy, I., 2012. Open quantum walks on graphs. Physics Letters A, 376(18), pp.1545-1548.

[43] Santos, R.A.M., Portugal, R. and Fragoso, M.D., 2014. Decoherence in quantum Markov chains. Quantum information processing, 13(2), pp.559-572.

[44] Sinayskiy, I. and Petruccione, F., 2014. Quantum optical implementation of open quantum walks. International Journal of Quantum Information, 12(02), p.1461010.

[45] Goolam Hossen, Y.H., Sinayskiy, I. and Petruccione, F., 2015. Non-reversal open quantum walks. in preparation.

[46] Bouwmeester, D. and Nienhuis, G., 1996. Measuring a single quantum trajectory. Quantum and Semiclassical Optics: Journal of the European Optical Society Part B, 8(1), p.277.

[47] Rohde, P.P., Brennen, G.K. and Gilchrist, A., 2013. Quantum walks with memory provided by recycled coins and a memory of the coin-flip history. Physical Review A, 87(5), p.052302.

[48] Sinayskiy, I. and Petruccione, F., 2012. Properties of open quantum walks on $\mathbb{Z}$. Physica Scripta, 2012(T151), p.014077.

[49] Roiter, Y. and Minko, S., 2005. AFM single molecule experiments at the solid-liquid interface: in situ conformation of adsorbed flexible polyelectrolyte chains. Journal of the American Chemical Society, 127(45), pp.15688-15689.

[50] Paul J. Flory, 1953. Principles of polymer chemistry. Cornell University Press.

[51] Flory, P.J., 1969. Statistical mechanics of chain molecules. Interscience.

[52] Rubinstein, M. and Colby, R., 2003. Polymers physics (Vol. 767). Oxford University Press.

[53] De Gennes, P.G., 1979. Scaling concepts in polymer physics. Cornell university press.

[54] Bhattacharjee, S.M., Giacometti, A. and Maritan, A., 2013. Flory theory for polymers. Journal of Physics: Condensed Matter, 25(50), p.503101.

[55] Mark, J.E., 2007. Physical Properties of Polymers Handbook. Springer.

[56] Isaacson, J. and Lubensky, T.C., 1980. Flory exponents for generalized polymer problems. Journal de Physique Lettres, 41(19), pp.469-471.

[57] Mandelbrot, B.B., 1983. The fractal geometry of nature/Revised and enlarged edition. WH Freeman and Co.

[58] Smailer, I., Machta, J. and Redner, S., 1993. Exact enumeration of self-avoiding walks on lattices with random site energies. Physical Review E, 47(1), p.262.

[59] Chakrabarti, B.K. ed., 2005. Statistics of linear polymers in disordered media. Elsevier.

[60] Blöte, H.W.J. and Hilhorst, H.J., 1983. Critical exponent of a directed self-avoiding walk. Journal of Physics A: Mathematical and General, 16(15), p.3687.